


SWEET BRIAR COLLEGE



3 2449 0412909 4



Digitized by the Internet Archive
in 2010 with funding from
Lyrasis Members and Sloan Foundation

<http://www.archive.org/details/newplatinumivmol00garc>

NEW PLATINUM (IV) MOLECULAR PROBES: SYNTHESIS,
CHARACTERIZATION, AND DNA BINDING SITES

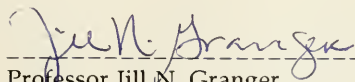
by

Stephanie Jocelyn Garcia

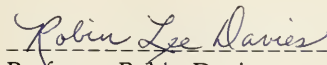
Department of Chemistry
Sweet Briar College

Date: April 30, 1997

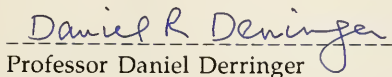
This senior honors thesis has been awarded Highest Honors.



Professor Jill N. Granger
Sweet Briar College



Professor Robin Davies
Sweet Briar College



Professor Daniel Derringer
Hollins College

**NEW PLATINUM(IV) MOLECULAR PROBES:
SYNTHESIS, CHARACTERIZATION,
AND DNA BINDING STUDIES**

*A Senior Honors Research Thesis
in the Department of Chemistry
Submitted to the Honors Committee
of Sweet Briar College*

by Stephanie Jocelyn Garcia

*In Partial Fulfillment of the Requirements
for the Honors Degree of
Bachelor of Science
in Biochemistry and Molecular Biology
May 1997*

Research Adviser:

Dr. Jill N. Granger, Sweet Briar College

Second Reader:

Dr. Robin L. Davies, Sweet Briar College

Outside Reader:

Dr. Daniel R. Derringer, Hollins College

For my parents, my big sis, and my grandparents
with all my love and thanks. I do it all for you.

Dedicated especially to grandpa
(I know you're proud and that
you'll always be watching over me).

ACKNOWLEDGMENTS

I take great pride in my work, but with humility, I offer thanks to all those who have helped me along the way and who made this senior thesis project possible. Thanks especially to my research adviser Dr. Jill N. Granger for all the guidance, for the exciting opportunity to do research, and for “making” me do things that are good for me (such as oral presentations). Thanks also to Dr. Robert Granger of Virginia Military Institute (VMI) for the optimism and project collaborations, especially with the syntheses. Dr. Robin Davies answered many questions throughout the year and offered support on behalf of the Biology Department of Sweet Briar College (SBC). To Dr. Daniel Derringer of Hollins College, thank you for helping to complete my thesis defense by graciously accepting to be my outside reader. Thanks to the Chemistry Department of SBC for the support and resources provided to make me feel “spoiled.” To the Honors Program of SBC, I am grateful for the opportunity to conduct senior honors thesis work that will prepare me for graduate school.

Several grants have made this project possible, including the SBC Faculty Grants-in-Aid; the VMI Faculty Grants-in-Aid; the Virginia Academy of Sciences Small Project Research Grant; and the Mednick Award from the Virginia Foundation of Independent Colleges. I also wish to acknowledge the SBC Summer Honors Fellowship and the VMI Chemistry Summer Research Fellowship which supported me during the summer of 1995.

I appreciate all the support and encouragement of my friends while I was frustrated or excited. Thanks for listening. Thanks especially to Jen for the HyperChem models, to Heather for teaching me some of the finer points of computer technology, and to Amanda and Natalie just for being around to keep me company in Guion all the time.

Finally, I am most grateful to my parents for all the love, encouragement, and support. Without them, such a wonderful education would not have been possible.

TABLE OF CONTENTS

page

viii LIST OF TABLES

ix LIST OF FIGURES

xii LIST OF ABBREVIATIONS

xiv ABSTRACT

1 SECTION 1: PROJECT SIGNIFICANCE

1 Section 1.1: Introduction

1 Section 1.2: Metal Complexes Studied

4 Section 1.3: DNA Structures

4 Section 1.4: Structural Tools

6 Section 1.5: Modes of DNA Binding

13 Section 1.6: Manipulation of Genetic Regulation

14 Section 1.7: Platinum

16 Section 1.8: Project Objectives

18 SECTION 2: PROJECT HISTORY

18 Section 2.1: Synthesis

20 Section 2.2: Characterization

20 Section 2.3: DNA Binding Studies

22 SECTION 3: CHEMICALS AND EQUIPMENT

23 SECTION 4: EXPERIMENTAL

23 Section 4.1: Synthesis

25 Section 4.2: DNA Binding Studies - Gel Electrophoresis

27 Section 4.2A: Gel electrophoresis comparison of (2) vs. control

28 Section 4.2B: Gel electrophoresis comparison of Ru(phen)_3^{+2} vs. Ru(dipy)_3^{+2} and Ru(phen)_3^{+2} vs. (2)

29 Section 4.2C: Gel electrophoresis as a method for topoisomerase I assay

33 Section 4.3: DNA Binding Studies - UV-Vis Absorption Spectroscopy

35 SECTION 5: RESULTS AND DISCUSSION

35 Section 5.1: Synthesis

40 Section 5.2: Preliminary DNA Binding Studies - Gel Electrophoresis

40 Section 5.2A: Gel electrophoresis comparison of (2) vs. control

43 Section 5.2B: Gel electrophoresis comparison of Ru(phen)_3^{+2} vs. Ru(dipy)_3^{+2} and of Ru(phen)_3^{+2} vs. (2)

page

46.....	Section 5.2C: Gel electrophoresis as a method for topoisomerase I assay
49.....	Section 5.3: Preliminary DNA Binding Studies - UV-Vis Absorption Spectroscopy
52.....	<u>SECTION 6: FUTURE RESEARCH</u>
52.....	Section 6.1: Continued Synthesis of Homoleptic Platinum(IV) Molecules
53.....	Section 6.2: DNA Binding Studies
53.....	Section 6.2A: Gel Electrophoresis
53.....	Section 6.2B: UV-Vis Absorption Spectroscopy
55.....	Section 6.2C: Cell Studies
55.....	Section 6.2D: Compilation of $M(N-N)_3$ Characteristics
56.....	<u>SECTION 7: CONCLUSIONS</u>
57.....	APPENDICES
57.....	Appendix A: Time Line Summary of Research
58.....	Appendix B: Calculation of pBR322 mM Nucleotides
59.....	Appendix C: Calculation of P/D
60.....	Appendix D: Chemical Characteristics of Platinum and Ruthenium
64.....	BIBLIOGRAPHY
70.....	VITA

LIST OF TABLES

<u>page</u>	<u>Table</u>	
2.....	1.1	DNA binding interactions have been studied and reported in the literature with these transition metals (M) as the centers in coordination complexes of the type $M(N-N)_3$ where the N-N ligand is a phenanthroline or phenanthroline derivative
26.....	4.1	Buffers
27.....	4.2	Stock Solutions of Metal Complexes
27.....	4.3	DNA Solutions
28.....	4.4	Composition of Gel Wells
31.....	4.5	Comparison of Topoisomerase I Assay Methods
32.....	4.6	Buffer Compositions for Topoisomerase I Assays
32.....	4.7	General Composition of Lanes in Topoisomerase I Assays
37.....	5.1	Microanalysis results for $Pt(DPK)Cl_4$ and $[Pt(phen)_3][PF_6]_4$ (compound (2))
42.....	5.2	Migration distances of Lambda Hind III fragments and pBR322 in control and compound (2) gels
45.....	5.3	Migration distances and percent change of the 5th fragment of Lambda Hind III and the 3rd band of pBR322 in A: control, B: $Ru(dipy)_3^{+2}$, C: $Ru(phen)_3^{+2}$, and D: (2) complex gels
49.....	5.4	Changes in A_{447} for $Ru(phen)_3^{+2}$

LIST OF FIGURES

<u>page</u>	<u>Figure</u>	
3.....	1.1.	Bidentate ligands (N-N) used for homoleptic and heteroleptic metal coordination complexes employed in DNA binding studies reported in the literature. The ligands investigated in this project include: 1,10-phenanthroline (phen); 4,7-dimethylphenanthroline (4,7-DMP); 2,9-dimethyl phenanthroline (2,9-DMP); 2,2'-dipyridyl (dipy); and di-2-pyridyl ketone (DPK).
3.....	1.2.	Representation of an octahedrally coordinated metal centered complex with three bidentate ligands, $M(N-N)_3$.
6.....	1.3.	Representation of left (Λ) and right (Δ) handed enantiomers of $M(N-N)_3$ compounds.
7.....	1.4.	DNA intercalation of Λ and Δ forms of $[Pt(N-N)_3]^{+4}$. As molecular probes, enantiomers may probe the handedness of DNA. The probes can interact with the DNA double helix by intercalation, groove binding, electrostatics, or various combinations of these modes of interaction.
8.....	1.5 a-d.	Molecular model of $Pt(phen)_3^{+4}$ interacting with the major groove of B-DNA, built using HyperChem. a) Representation of intercalation between the base pairs of DNA; one of the flat aromatic ligands “slips” between the DNA base pairs. b) This 90° rotation of figure 1.5 a. depicts the ancillary ligands clashing with the DNA backbone. c) This simplified representation of figure 1.5 a. depicts intercalation between two DNA base pairs. The flatness of the aromatic intercalative ligand enhances intercalation between the base pairs. This property arises from the presence of nitrogen which is also present in the DNA bases, making them flat as well. d) This model depicts the ancillary ligands clashing with a two base pair region of the DNA backbone, as in figure 1.5 b. The probe-DNA interaction depends on the orientation, steric hinderances, and electrostatics of the two ancillary ligands in addition to the properties of the intercalating ligand.

19.....	2.1.	Reaction for the synthesis of $\text{Pt}(\text{DPK})\text{Cl}_3$.
19.....	2.2.	Proposed structures of $\text{Pt}(\text{N-N})_3^{+4}$ compounds studied in this project: $\text{Pt}(\text{phen})_3^{+4}$ (2); $\text{Pt}(\text{dipy})_3^{+4}$ (3); and $\text{Pt}(4,7\text{-DMP})_3^{+4}$ (4).
24.....	4.1.	Scheme 1: Specific reactions for the synthesis of homoleptic $\text{Pt}(\text{N-N})_3$ complexes.
34.....	4.2.	Scheme 2: UV-Vis experimental plan. Matching cuvettes were used. 10 mM phosphate buffer was used as the blank. To both cuvettes, the same amount of metal complex was added and the A_{447} was obtained. For cuvette 1, 11 μl additional buffer was added and the A_{447} was again obtained. For cuvette 2, 11 μl of 23 mM CT-DNA was added and the A_{447} was obtained.
35.....	5.1.	X-ray crystal structure of $[\text{Pt}(\text{phen})\text{Cl}_3]$. Selected bond lengths and angles: N(1)-Pt 2.037 Å; N(10)-Pt 2.042 Å; Cl(1)-Pt 2.317 Å; Cl(2)-Pt 2.302 Å; Cl(3)-Pt 2.299 Å; Cl(4)-Pt 2.309 Å; N(1)-Pt - N(10) 80.6°; Cl(2)-Pt -Cl(3) 89.05°; Cl(2)-Pt -Cl(4) 91.6°; Cl(1)-Pt -Cl(2) 91.6°; Cl(1)-Pt -Cl(3) 90.93°; Cl(3)-Pt -Cl(4) 91.36°; N(1)-Pt -Cl(3) 95.1°; N(10)-Pt -Cl(2) 95.3°.
36.....	5.2.	X-ray crystal structure of $[\text{Pt}(\text{di-2-pyridyl ketal})\text{Cl}_3]$. This is the tautomer of the synthesized $[\text{Pt}(\text{di-2-pyridyl ketone})\text{Cl}_4]$ product.
36.....	5.3.	Representation of tautomerization of $[\text{Pt}(\text{2'-dipyridyl ketone})\text{Cl}_4]$ and $[\text{Pt}(\text{di-2-pyridyl ketal})\text{Cl}_3]$.
38.....	5.4.	The IR spectrum of compound (3) superimposed on the IR spectra of compound (2) and $\text{Ru}(\text{phen})_3[\text{PF}_6]_2$ for comparison of the major peaks. The striking similarities suggest analogous compounds.
42.....	5.5.	The 1% non-denaturing agarose gels above are the (2) gel (0.94 μM) and the control gel (no metal complex present). The outer lanes are λ Hind III (0.5 μg) and the inner lanes are pBR322 (0.2 μg). Migration distances are given in Table 5.2.
44.....	5.6.	1% non-denaturing agarose gels: control (A), $\text{Ru}(\text{dipy})_3^{+2}$ (B), $\text{Ru}(\text{phen})_3^{+2}$ (C). Lanes 1, 5: λ Hind III; Lanes 2, 3, 4: pBR322.
44.....	5.7.	1% non-denaturing agarose gels: control (A), $\text{Ru}(\text{phen})_3^{+2}$ (C), and compound (2) (D). Lanes 1, 5: λ Hind III; Lanes 2, 3, 4: pBR322.
47.....	5.8.	Topoisomerase I assay. 1% non-denaturing agarose gel with TBE running buffer and standard topo I reaction buffer: lane 1 = λ Hind

- III; lane 2 = pBR322 + Bam HI (linear pBR322); lane 3 = pBR322; lane 4 = pBR322 + 1 unit topo I; lanes 5-10 = pBR322 + 1 unit topo I + decreasing concentrations of $\text{Ru}(\text{dipy})_3^{+2}$ (~10 μM - ~2 μM).
- 48.....5.9. Gel electrophoresis of pBR322 in the absence and presence of topo I and $\text{Ru}(\text{phen})_3^{+2}$ with two different reaction buffers varying in $[\text{Mg}^{+2}]$. Lane 1 = λ Hind III; lane 2 = pBR322 linearized by Bam HI; lanes 3 = pBR322; lane 4 = pBR322 + topo I (2 units); lane 5 = pBR322 + topo I (2 units) and 1 μM $\text{Ru}(\text{phen})_3^{+2}$; and lane 6 = pBR322 + topo I and 10 μM $\text{Ru}(\text{phen})_3^{+2}$ in BL ($[\text{Mg}^{+2}] = 0$); lanes 7-10 = same as 3-6 but in BL ($[\text{Mg}^{+2}] = 1.5 \text{ mM}$).
- 50.....5.10. UV-Vis Absorption spectrum of $\text{Ru}(\text{phen})_3^{+2}$ in the absence of CT-DNA. The top spectrum is with 500 μl total volume, concentration approximately 12.4 μM . The bottom spectrum is with 511 μl total volume, concentration approximately 11.4 μM . A 7.8% change in the A_{447} is observed for concentration changes.
- 50.....5.11. UV-Vis Absorption spectrum of $\text{Ru}(\text{phen})_3^{+2}$ in the absence and presence of CT-DNA. The top spectrum is in the absence of CT-DNA with 500 μl total volume. The bottom spectrum is in the presence of CT-DNA with 511 μl total volume. A total change of 14.0% in the A_{447} is observed for concentration changes and CT-DNA binding effects. Based on the results shown in figure 5.10 above, a 7.8% change is accounted for by change in concentration; thus a 6.2% change in the A_{447} is observed CT-DNA binding effects only.

LIST OF ABBREVIATIONS

\AA = Angstrom = 10^{-10} m

$A_{\lambda_{\text{max}}}$ = absorbance at λ max

A_{pres} = absorbance at λ max in the presence of CT-DNA

A_{abs} = absorbance at λ max in the absence of CT-DNA

% ΔA = percent change in absorbance at λ max in the presence and absence of CT-DNA

$\text{Ag}_3(\text{citrate})$ = trisilver citrate

B1 = buffer 1

B2 = buffer 2

B3 = buffer 3

BL = low salt concentrations buffer

bp = base pair

BS = standard suggested reaction buffer

BSA = bovine serum albumin

c = concentration of ion

CT-DNA = calf thymus DNA

dipy = 2,2'-dipyridyl

2,9-DMP = 2,9-dimethylphenanthroline

4,7-DMP = 4,7-dimethylphenanthroline

DMSO = dimethyl sulfoxide

DNA = deoxyribonucleic acid

DPK = 2,2' dipyridyl ketone

DTT = dithiothreitol

Δ , Λ = right and left enantiomers

EDTA = disodium ethylenediaminetetraacetic acid

$\epsilon_{\lambda_{\text{max}}}$ = absorptivity coefficient at λ max

ether = diethyl ether

EtOH = ethanol

I = ionic strength

IR = infrared

K_2PtCl_6 = potassium hexachloroplatinate(IV)

KPF_6 = potassium hexafluorophosphate

λ Hind III = bacteriophage lambda DNA cut with the restriction endonuclease Hind III

LB = loading buffer

M = transition metal center

$\text{M}(\text{N}-\text{N})_3$ = tris-substituted, octahedrally -coordinated metal center compounds

MW = molecular weight

NMR = nuclear magnetic resonance

N-N = diimine bidentate ligands

nt = nucleotides

P/D = molar concentration phosphates in DNA per molar concentration of dye. Dye refers to metal complex.

phen = 1,10-phenanthroline

Pt(II) = platinum(II)

Pt(IV) = Platinum(IV)

Pt(phen)Cl₄ = tetrachloro-1,10-phenanthroline platinum(IV)

Pt(DPK)Cl₃ = trichloro-di-2-pyridylketalplatinum(IV)

Pt(DPK)Cl₄ = tetrachloro-di-2-pyridylketoplatinum(IV)

[Pt(phen)(DPK)Cl₂]Cl₂ = **(1)** = dichloro-2,2'-dipyridylketone-1,10-phenanthroline-platinum(IV) chloride

[Pt(phen)₃](PF₆)₄ = **(2)** = tetra(hexafluorophospho)-tris(1,10-phenanthroline)platinum(IV)

[Pt(DMP)₃](PF₆)₄ = **(3)** = tetra(hexafluorophospho)-tris(4,7-dimethyl-1,10-phenanthroline)platinum(IV)

[Pt(dipy)₃](PF₆)₄ = **(4)** = tetra(hexafluorophospho)-tris(2,2'-dipyridyl)platinum(IV)

ppt = precipitate

RB = running buffer

RE = restriction endonucleases

rpm = revolutions per minute

Ru(dipy)₃⁺² = tris(2,2'-dipyridyl)ruthenium(II)

Ru(phen)₃⁺² = tris(1,10-phenanthroline)ruthenium(II)

SBC = Sweet Briar College

TAE = tris-acetate buffer

TB1 = topoisomerase buffer 1

TB2 = topoisomerase buffer 2

TBE = tris-borate buffer

TIP = Thinking in Progress discussion

topo I = topoisomerase I

Tris = tris[hydroxymethyl]aminomethane (Trizma base)

UV = ultraviolet

VMI = Virginia Military Institute

Z = charge

ABSTRACT

Garcia, Stephanie Jocelyn. B.S., Sweet Briar College, May 1997. New Platinum(IV) Molecular Probes: Synthesis, Characterization, and DNA Binding Studies. Research Adviser: Jill N. Granger.

Transition metal complexes have important biological applications, such as the potential to probe DNA secondary structure and the potential to manipulate DNA by acting as artificial nucleases. This project focuses on the characteristics of octahedrally coordinated metal centered complexes. In particular, the synthesis, characterization, and DNA binding of platinum(IV) (Pt(IV)) molecular probes are investigated. Six compounds have been either fully or partially characterized: tetrachloro-1,10-phenanthroline-platinum(IV) $[\text{Pt}(\text{phen})\text{Cl}_4]$; trichloro-di-2-pyridylketalplatinum(IV) $[\text{Pt}(\text{DPK})\text{Cl}_3]$; dichloro-2,2'-dipyridylketone 1,10-phenanthroline platinum(IV) chloride $[\text{Pt}(\text{phen})(\text{DPK})\text{Cl}_2]\text{Cl}_2$ (**1**); tetra(hexafluorophospho)-tris(1,10-phenanthroline)platinum(IV) $[\text{Pt}(\text{phen})_3](\text{PF}_6)_4$ (**2**); tetra(hexafluorophospho)-tris(4,7-dimethyl-1,10-phenanthroline)platinum(IV) $[\text{Pt}(\text{DMP})_3](\text{PF}_6)_4$ (**3**); and tetra(hexafluorophospho)-tris(2,2'-dipyridyl)platinum(IV) $[\text{Pt}(\text{dipy})_3](\text{PF}_6)_4$ (**4**). From gel electrophoresis studies, it was shown that compound (**2**) retards the migration of supercoiled pBR322 DNA and bacteriophage lambda DNA digested with the restriction endonuclease Hind III. A UV-Vis absorption spectroscopic method developed with $\text{Ru}(\text{phen})_3^{+2}$ confirmed that the metal complex interacted with calf thymus DNA. In preliminary experiments this method was applied to compound (**2**) and a decrease in the absorption at lambda max ($\lambda_{\text{max}} = 508$ nm) was suggested.

SECTION 1: PROJECT SIGNIFICANCE

Section 1.1: Introduction

Transition metal complexes can be used as tools in molecular biology applications; such applications include the ability to probe unusual DNA structures and to manipulate DNA by acting as artificial enzymes (Tullius, 1989). Of particular interest is the design and synthesis of metal complexes that recognize and bind to DNA and the understanding of this interaction. Many different metal complexes are possible, but this project focuses on the simple transition metal chelate complexes. By virtue of the metal center, these complexes have a rigid structure. Therefore, one potential function of these metal chelate complexes is as molecular probes which possess the potential to aid in the analysis of DNA structure. By virtue of their characteristic size and shape, molecular probes exhibit site specificity when interacting with DNA. In addition, the linkage of this site specificity to the chemical action of the metal center may result in site specific artificial endonucleases which nick and cleave DNA. This feature may have an important application in the Human Genome Project because these complexes would cleave the genome into manageable fragments for analysis by recognizing more specific sites on the DNA than existing restriction endonucleases (RE) (i.e., 15 base pairs compared to 4-8 base pairs for existing RE's). Furthermore, the structural properties of these molecular probes offer applications in the rational design of DNA targeting drugs by relaying information about the structure of the DNA at the target site.

Section 1.2: Metal Complexes Studied

Useful metal chelate complexes (also termed coordination complexes) that have been studied as molecular probes or artificial endonucleases include as a general class octahedrally-coordinatedⁱ,

ⁱ An octahedral complex has six binding sites at the corners of an octahedron, with the metal ion at the center.

metal-centered complexes with three bidentate ligandsⁱⁱ. These coordination complexes can be symbolically represented as complexes of type $M(N-N)_3$, where M represents a transition metal center (table 1.1) and N-N represents a bidentate ligandⁱⁱⁱ (figure 1.1). The octahedral coordination of three of the ligands results in a propeller-like complex (figure 1.2). Tris(phenanthroline) ruthenium(II) ($Ru(phen)_3^{+2}$) is one of the most recognized complexes of the type $M(N-N)_3$ as a DNA binding agent and as a photochemically activated nuclease.

Table 1.1. DNA binding interactions have been studied and reported in the literatureⁱⁱ with these transition metals (M) as the centers in coordination complexes of the type $M(N-N)_3$ where the N-N ligand is a phenanthroline or phenanthroline derivative

<u>M</u>	<u>Name</u>
Co	cobalt
Cr	chromium
Cu	copper
Fe	iron
Ni	nickel
Os	osmium
Rh	rhodium
Ru	ruthenium

ⁱⁱ References include: Anderson (1973); Barton et al. (1982, 1983, 1984, 1985, 1986, 1989); Fleisher et al. (1986); Friedman, et al. (1990,1991); Goldstein et al. (1986); Haq, et al. (1995); Kauffman, Takahashi (1966); Kelly et al. (1985); Krotz, et al. (1993); Kumar et al. (1985); Mei, Barton (1986, 1988); Pope, Sigman (1984); Pyle et al. (1985, 1989); Rehmann, Barton (1990); Satyanarayana et al. (1992, 1993); Sigman (1986); Yamagishi (1984).

ⁱⁱⁱ A ligand is a Lewis base attached to the metal center, a Lewis acid. A bidentate ligand can simultaneously occupy two sites on the metal center.

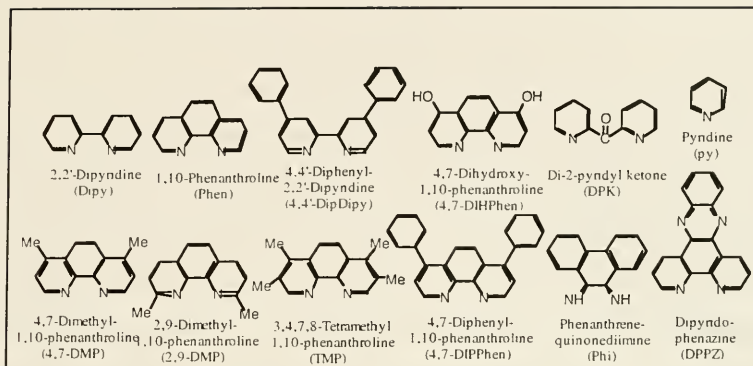


Figure 1.1. Bidentate ligands (N-N) used for homoleptic and heteroleptic metal coordination complexes employed in DNA binding studies reported in the literatureⁱⁱ. The ligands investigated in this project include: 1,10-phenanthroline (phen); 4,7-dimethylphenanthroline (4,7-DMP); 2,9-dimethylphenanthroline (2,9-DMP); 2,2'-dipyridyl (dipy); and di-2-pyridyl ketone (DPK).

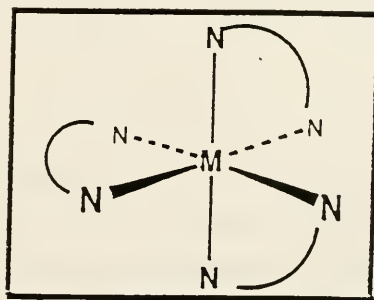


Figure 1.2. Representation of an octahedrally coordinated metal centered complex with three bidentate ligands. $M(N-N)_3$.

Section 1.3: DNA Structures

DNA exists in various structural forms including B-DNA, A-DNA, and Z-DNA. The shape of the DNA depends on the sequence of the bases. B-DNA is the most commonly known conformation. It is a right handed, antiparallel double helix with a wide deep major groove and a narrow deep minor groove. Typically, B-DNA has 10 base pairs per helical turn, 36° helical twist per base pair, and a 34 Å helix pitch (rise per turn). A-DNA is also right handed, but has a narrow deep major groove and a wide shallow minor groove. A-DNA has 11 base pairs per helical turn, 33° helical twist per base pair, and a 28 Å helix pitch. Z-DNA is left handed, antiparallel, and has a characteristic zigzag helix due to its alternating pyrimidine-purine sequence. This results in a flat major groove and a narrow deep minor groove. Z-DNA has 12 base pairs per helical turn, 60° helical twist per base pair, and a 45 Å helix pitch. In addition to these “typical” DNA structures are other secondary structures including single stranded DNA, triple stranded DNA, loops, cruciforms, hairpins, kinks and bends, and left-handed helical segments within right handed DNA. DNA secondary structure is assumed to play a role in gene regulation, most notably the supercoiling which affects DNA transcription. Probing the structure of DNA may be used to study the extent of these unusual structures as well as the handedness in the biological function of the DNA (Barton, 1986).

Section 1.4: Structural Tools

To expand on the supply of natural enzymes that have specificity for certain DNA structures, some research has centered on the design and synthesis of new molecules that probe structure to yield desired structural information^{iv}. In particular, metal complexes have been used because the geometry of the molecule and the structure of the ligand can be readily manipulated to build specific

^{iv} Tullius, 1989; Barton et al. 1982, 1983, 1984, 1985, 1986, 1989; Chow & Barton, 1990; Haworth et. al, 1991; Krotz, et al., 1993; Mei, et al. 1988, 1986; Pope and Sigman, 1984; Pyle et al., 1989; Rehmann & Barton, 1990; Satyanarayana et al., 1993; and Sitlani, et al., 1993.

recognition features. In addition, metals are reactive (redox reactions, photochemical reactions) which is important in the cleavage of DNA. For example, cobalt cleaves DNA by a photochemical reaction (Tullius, 1989). Another important feature of metal ions is that they show biological activity such as mutagenicity and cytotoxicity because they often coordinate directly to the nucleotide bases of the DNA. The phosphate anions along the backbone coupled to the nitrogen lone pairs on the purines and pyrimidines provide favorable sites for transition metal coordination. This makes DNA a good ligand for metals (Barton, 1986).

Molecule chirality of metal complexes is thought to be complementary to DNA (Barton, 1986). A molecule is considered chiral if the isomers of the molecule are non-superimposable mirror images of each other that share identical chemical properties; these isomers are termed enantiomers (figure 1.3). Several studies have focused on the binding preference of tris substituted phenanthroline (and phen derivatives) metal complex enantiomers for right and left handed DNA using varying methods^v. These $M(N-N)_3$ complexes were shown to bind to different forms of DNA but the mode of binding remains an issue for debate.

^v Barton et al., 1982; 1983; 1984; 1985; 1986; and 1989; Haq, et al., 1995; Krotz, et al., 1993; Mei, et al., 1988 and 1986; Rehmann and Barton, 1990; Satyanarayana, et al. 1992, 1993; and Yamagishi, 1984.

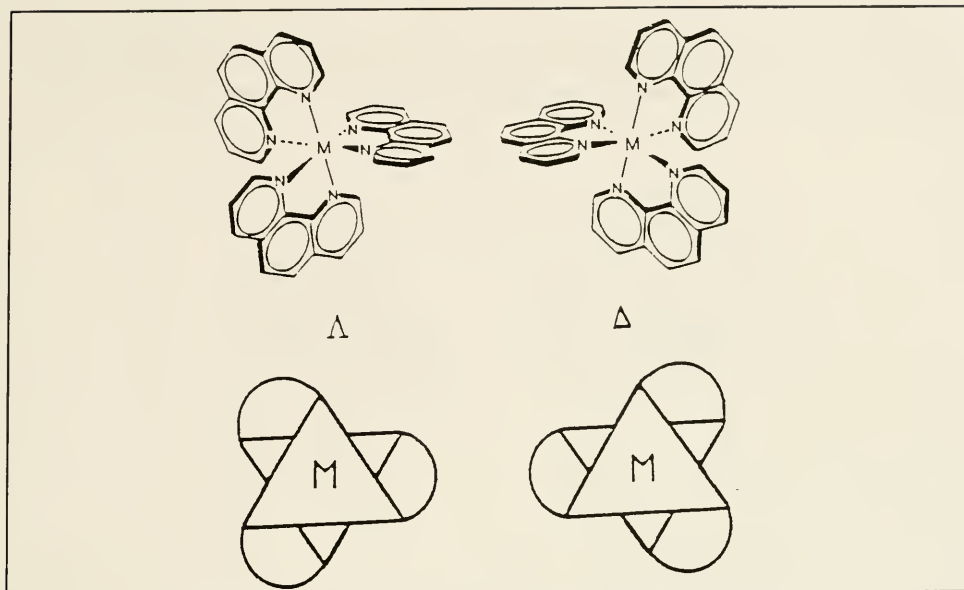


Figure 1.3. Representation of left (Λ) and right (Δ) handed enantiomers of $M(N-N)_3$ compounds.

Section 1.5: Modes of DNA Binding

These molecules have been shown to bind to DNA at shape specific sites through various modes of binding. These modes of binding can be covalent, hydrophobic, electrostatic, and/or mediated by hydrogen bonding. In electrostatic binding, the negative charge of the phosphate groups along the DNA backbone attracts the positively charged metal complexes. In surface binding or groove binding, the metal complex associates itself into the grooves of DNA via steric interactions. Some of the enantiomers exhibit a preference for left or right handed DNA. Groove binders prefer structures of complementary symmetry (like a right hand interlocks with a left hand) (Barton, 1986). In intercalation, one of the flat aromatic ligands is perpendicularly inserted between the stacked base pairs of the DNA while the other two ligands lie in the groove of the DNA (figure 1.4 and 1.5 a-d) (Barton, 1984). In contrast to groove binders, intercalators prefer helices of like symmetry (right with right) (Barton, 1986). The ancillary ligands, the steric

hindrance associated with each ligand, and the symmetry of the molecules impart shape specificity such that by binding at shape specific places, the probes can “fit” into the DNA, like a puzzle piece into a puzzle.

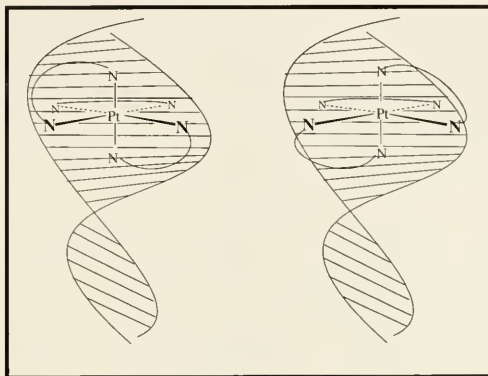


Figure 1.4. DNA intercalation of Λ and Δ forms of $[\text{Pt}(\text{N-N})_3]^{4+}$. As molecular probes, enantiomers may probe the handedness of DNA. The probes can interact with the DNA double helix by intercalation, groove binding, electrostatics, or various combinations of these modes of interaction.

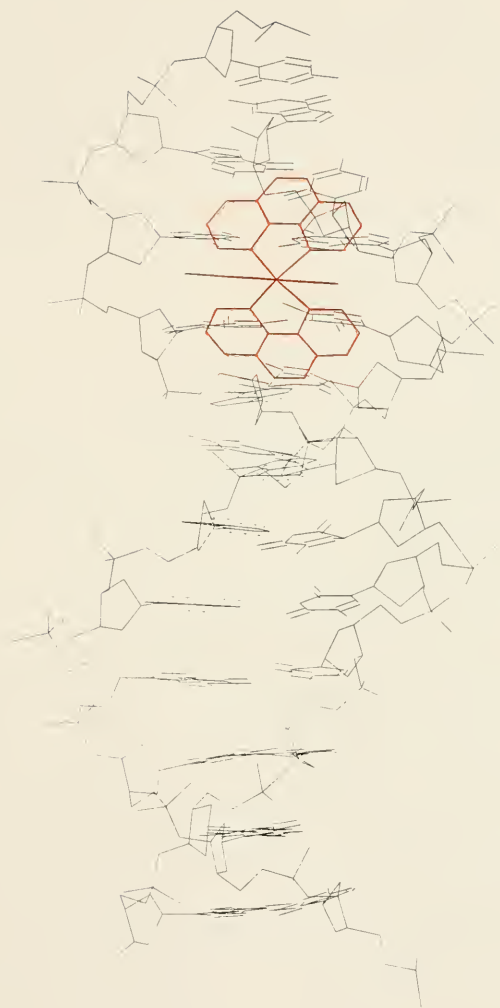


Figure 1.5. Molecular model of $\text{Pt}(\text{phen})_3^{4+}$ interacting with the major groove of B-DNA, built using HyperChem. **a)** Representation of intercalation between the base pairs of DNA; one of the flat aromatic ligands “slips” between the DNA base pairs.

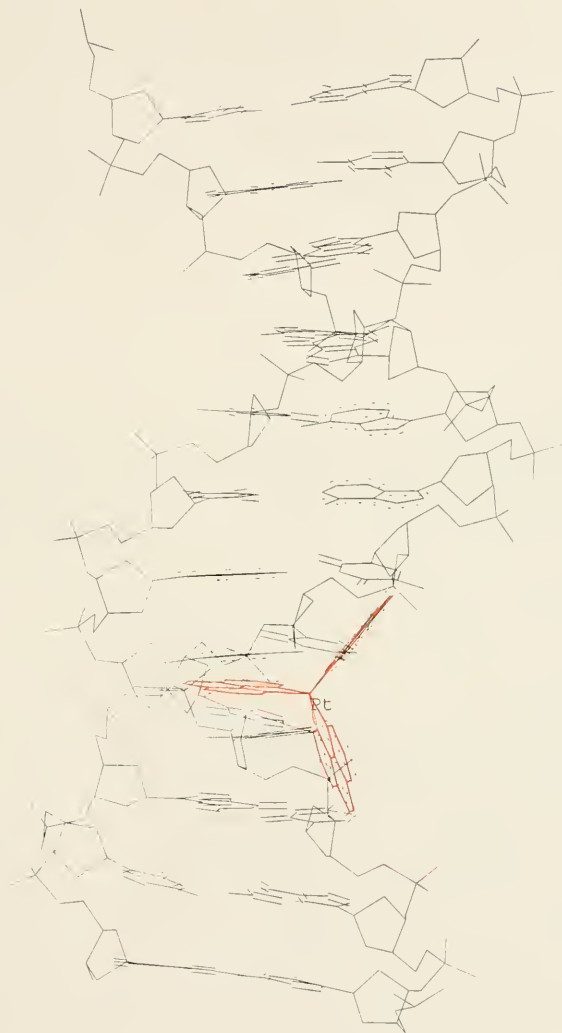


Figure 1.5 b) This 90° rotation of figure 1.5 a. depicts the ancillary ligands clashing with the DNA backbone.

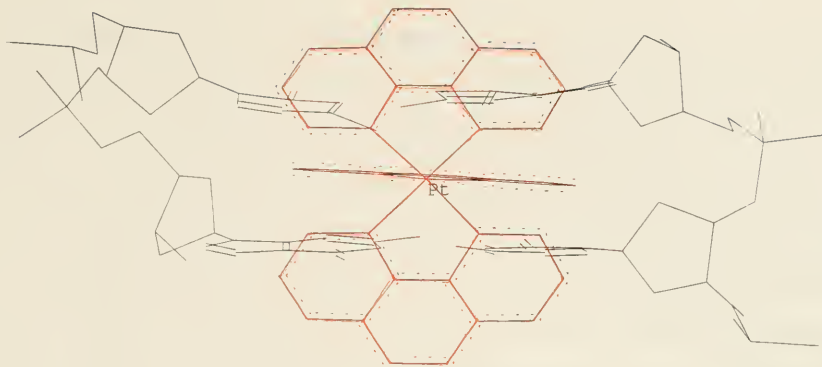


Figure 1.5 c) This simplified representation of figure 1.5 a. depicts intercalation between two DNA base pairs. The flatness of the aromatic intercalative ligand enhances intercalation between the base pairs. This property arises from the presence of nitrogen which is also present in the DNA bases, making them flat as well.



Figure 1.5 d) This model depicts the ancillary ligands clashing with a two base pair region of the DNA backbone, as in figure 1.5 b. The probe-DNA interaction depends on the orientation, steric hinderances, and electrostatics of the two ancillary ligands in addition to the properties of the intercalating ligand.

Knowing the structure of the DNA is useful in the rational design of new drugs which target DNA. First, knowing the structure of the probe and second, understanding the probe-DNA interaction aids in the determination of the DNA structure at the specific sites where the probes bind, like a round peg indicates the shape of a round hole. For these types of metal chelated complexes to be of use as practical molecular probes of DNA structure, the number and modes of DNA interaction need to be determined. However, determination of the mode of binding is an issue of controversy. While some authors^{vi} claim that the molecular probes bind via intercalation, more recent articles propose that this has not been unambiguously proven. Rather, these authors suggest that the mode of interaction is a combination of partial insertion, groove binding, and electrostatics.

According to a brief compilation of molecular probe history, Satyanarayana, Dabrowiak, and Chaires (1993) showed the mode of DNA binding to be a matter of controversy. In 1976, Norden and Tjerneld showed that $\text{Fe}(\text{dipy})_3^{+2}$ bound to DNA in an enantioselective manner, and suggested that intercalation was possible. Methods of analysis they used included linear dichroism (LD) and circular dichroism (CD). Pioneering work by Barton and co-workers concluded that $\Delta\text{-Zn}(\text{phen})_3^{+2}$ bound preferentially to right handed DNA by intercalation (Barton et al., 1982). Later investigations involving unwinding studies with closed circular DNA and absorption and fluorescence spectroscopies suggested that both isomers of $\text{Ru}(\text{phen})_3^{+2}$ intercalate between the base pairs of DNA. This was supported by a small (2 nm) hypochromic effect when the ruthenium complexes bound DNA as well as an increase in the fluorescence lifetimes (Barton et al., 1983, 1984). Kelly et al. (1985) confirmed that racemic $\text{Ru}(\text{phen})_3^{+2}$ unwinds closed circular pBR322 DNA using a topoisomerase I assay. Further, an increase in the melting temperature of an oligonucleotide that was similar to that effect observed with the classic intercalator ethidium bromide suggested the complex bound by intercalation. Yamagishi (1984) concluded, using electric dichroism, that $\Delta\text{-Ru}(\text{phen})_3^{+2}$ intercalated while $\Lambda\text{-Ru}(\text{phen})_3^{+2}$ bound electrostatically. In

^{vi} Specific references are given throughout the body of this section.

1986, Barton et al. studied the binding of each enantiomer to oligonucleotides of various compositions and structures by equilibrium dialysis and photophysical methods. They concluded that each enantiomer exhibited both intercalation and surface binding.

The possibility was raised of partial insertion of one phenanthroline ring and electrostatic binding of the complex in the major groove. This was supported by molecular modeling and energy minimization (Barton et al., 1984; Kelly et al., 1985; Haworth et al., 1991; and Satyanarayana et al., 1993). In partial insertion, intercalation is blocked by the clashing of the ancillary ligands with the DNA backbone (figure 1.5 b, and 1.5 d).

In contrast, Norden and co-workers^{vii} concluded that each enantiomer bound to DNA by a single mode, neither of which was intercalation. This was supported by linear dichroism and spectroscopic studies. Independent two dimensional NMR (nuclear magnetic resonance spectroscopy) studies further supported this and additionally proposed that binding occurred in the minor groove (Eriksson et al., 1992 in Satyanarayana et al., 1993). A later NMR study by Rehmann and Barton (1990) concluded $\Delta\text{-Ru(phen)}_3^{+2}$ prefers intercalation while $\Lambda\text{-Ru(phen)}_3^{+2}$ prefers surface binding in the minor groove. Furthermore, a preliminary report by Satyanarayana et al.(1992) suggested each enantiomer has a single binding mode, which is not intercalation. The interaction with DNA was proposed to be predominantly electrostatic based on the salt dependency of the complexes as DNA binding agents.

Satyanarayana and co-workers (1993) studied the mode and specificity of binding for Ru(phen)_3^{+2} enantiomers with DNA. They reported that, in contrast to the published results of Barton et al.(1989, 1986, 1984, 1983), the enantiomers did not exhibit significant selectivity for right handed B-DNA nor left handed Z-DNA. Results from fluorescence measurements, thermal melting experiments, equilibrium dialysis, and/or viscosity studies indicated that the complexes bind weakly to DNA, have modest base specificity, and cannot discriminate between such radically different conformations of DNA as B-DNA and Z-DNA. Based on these results, the potential of

^{vii} From Satyanarayana et al., 1993.

these ruthenium enantiomers as specific probes is limited since useful probes must have a high affinity for a specific site in the DNA. However, as Satyanarayana et al. (1993) pointed out, the characteristics exhibited by these coordination compounds impart potential usefulness as nonspecific footprinting reagents.

Section 1.6: Manipulation of Genetic Regulation

Some $M(N-N)_3$ molecular probes have the potential to act as artificial nucleases that cut the DNA at the sites where they bind; these binding sites are governed by the structure as well as the charge of the molecular probe. One example of a $M(N-N)_3$ complex that was shown to act as an artificial nuclease is bis(1,10-phenanthroline)copper(I), discovered by Sigman and co-workers (1979)^{viii} as the first artificial nuclease of this type. Molecular probes of the type $M(N-N)_3$ with different metal centers or different ligands bind and cleave DNA differently based on subtle distinctions in the structure of the metal and the ligands and on the reactivity of the metal center. The reactivity of the metal center reacts to cleave the DNA via photochemical cleavage or attack by hydroxyl radicals. This process can be used to map the DNA; that is, to determine the order and location of genes on the chromosomes and ultimately to determine the sequence of the DNA base pairs. This mapping process is also known as DNA footprinting. Footprinting analysis identifies the binding sites of drugs and proteins on DNA. This process has an important role in the identification of new types of DNA sequence level “smart drugs” (Goodisman and Dabrowiak, 1992).

As artificial endonucleases, these coordination compounds can augment natural restriction endonucleases (RE) which have “cutting and pasting” functions essential to recombinant DNA technology. Natural RE are limited in specificity of recognition since they usually have recognition sites 4-6 base pairs in length. The specificity offered by RE's of this length are adequate for cutting plasmid and viral DNA which are small genomes (2000-4000 bp for some plasmids and

^{viii} From Satyanarayana et al., 1993.

some viruses) compared to the genome size of higher organisms which are much larger (3 billion bp for humans). Therefore, cutting of an entire genome such as the human genome is a much more complex process. Reagents with longer recognition sites would yield a manageable number of fragments in the initial digest facilitating the mapping and sequencing of the human genome (Tullius, 1989). These fragments could then be further processed with less specific reagents. In fact, the currently available RE with 8 bp recognition sequences (e.g., Not I) are used extensively in genomic research. Thus, the development of new molecular probes with larger recognition sequences could potentially be a useful tool for the Human Genome Project.

Section 1.7: Platinum

This project focuses on the synthesis and DNA binding studies of Pt(IV) centered complexes analogous to the type $M(N-N)_3$ represented in the literature. These new Pt(IV) coordination compounds are interesting in and of themselves for the study of coordination chemistry. Platinum also has the advantage of being biologically important and this may contribute to the generation of new chemotherapeutic drugs. Because platinum is a transition metal, it is important to recall certain features of transition metals.

Transition metals have three general properties: their ability to form numerous complexes, their action as catalysts, and their extensive range of oxidation numbers. Transition metals often have more than one stable oxidation state, each having a different charge associated with it. The transition metals are also known as d-block members because they have atoms with electrons occupying the d-orbitals according to the building up principle^{ix}. Because the d-orbital electrons of transition metals are bound more strongly than the valence s-orbital electrons, the valence s electrons are lost first as one of these atoms becomes a cation, followed by the loss of a variable number of d electrons. The number of electrons lost results in oxidation states in which the effective charge is the oxidation number. The number of atoms bound to the metal center is known

^{ix} According to the building up principle, the orbitals are filled $1s < 2s < 2p < 3s < 3p < 4s < 3d \dots$ etc.

as the coordination number of the complex. The most common coordination numbers are four and six. Those complexes with a coordination number of six often form octahedral complexes whereas those with coordination number of four form tetrahedral or square-planar complexes.

Platinum has two common oxidation states, platinum(IV) (Pt(IV)), a +4 oxidation state, and platinum(II) (Pt(II)), a +2 oxidation state. Platinum(IV) has a coordination number of six so has six binding sites (therefore a maximum of three bidentate ligands can bind). It is thus octahedral (like an eight sided die). Platinum(II), in contrast, has a coordination number of four so has only four binding sites (binding only two bidentate ligands) and is thus square planar (like a sheet of paper).

Pt(II) has a rich and biologically important history as the metal center in the well-known chemotherapeutic drug *cis*-platin^x. Furthermore, other Pt(IV) molecules such as iproplatin and tetraplatin are being studied as more effective and less toxic drugs for chemotherapy ("new and improved" *cis*-platin drugs)^{xi}. Since Pt(IV) is structurally (conformationally) distinct from Pt(II) based on geometry, size, charge, and mode of interaction, molecules with Pt(IV) centers, which are octahedrally coordinated complexes, will bind in a different manner to DNA and thus will offer distinct information regarding DNA structure-function relationships. It is therefore important to investigate the synthesis and potential biological uses of platinum in all forms.

The significance of Pt(IV) centered molecules is important. First, Pt(N-N)₃⁺⁴ compounds are not well represented in the list of metal centers studied to date. Thus, information about its structure, chemistry, and DNA interactions is presently limited. Indeed, the "first isolated homoleptic organoplatinum(IV) compound ([Pt(C₆Cl₅)₄])" only recently appeared in the literature (Fornies et al., 1995). The lack of synthesis of Pt(IV) molecules is possibly due to the high charge

^x Discovered by Stephen Lippard; Bradley et al., 1992; Pinto et al., 1986.

^{xi} Bramwell, et al., 1985; Chaney et al., 1991; Choi et al., 1988; Defais et al., 1990; Eastman, 1987; Edwards, 1988; Kelland et al., 1992; Novakova, et al., 1995; Pendyala, et al., 1988; Rahman et al., 1988; Rotondo, et al., 1983; Vrana et al., 1986; Yarema et al., 1994.

density^{xii}, making Pt(IV) complexes difficult to solvate. In fact, one of the major hurdles encountered in this project in the synthesis of new tris-substituted Pt(IV) complexes has been the lack of solubility of the intermediates (i.e., mono and bis-substituted Pt(IV) centers did not dissolve in solvents, including DMSO). Solubility problems for the tris-substituted complexes have been serendipitously overcome, possibly because of enhanced symmetry. Second, platinum(IV) analogs should have different size-shape specificities when interacting with DNA compared to analogous M(N-N)₃ complexes with various metal centers and ligands. One reason for this is because the ionic radius, the contribution of an element to the distance between neighboring ions in a solid ionic compound, is characteristic for elements. For example, the ionic radius of platinum(IV) is small compared to ruthenium(II) (another octahedral metal ion). It would thus be expected that the distance between neighboring ions associated with the Pt(IV) is less than that for Ru(II). Third, because Pt(IV) has a +4 charge and DNA is negatively charged (at the phosphates), Pt(IV) complexes should have stronger electrostatic interactions with the DNA compared to the M(0), M(+1), and M(+2) analogs studied thus far.

Section 1.8: Project Objectives

The long term objective of this project is to develop a series of new tris-substituted Pt(IV) centered octahedrally-coordinated molecules to be used as site selective DNA binding probes, as artificial endonucleases used for DNA fingerprinting, or as potential therapeutic drugs. The long range objective is further broken down into the following goals:

- a) Synthesize, characterize and obtain X-ray crystal structures for a series of diimine tris-substituted Pt(IV) centered molecules.

^{xii} As a period 6 transition metal, platinum is among the densest elements of the period due to the lanthanide contraction effect which reduces the atomic radii of elements following the lanthanide series. This arises from the poor shielding ability of the f electrons present in the lanthanides that tends to increase the nuclear charge by pulling

- b) Perform DNA binding studies of the molecules with selected DNA strands including pBR322 and calf thymus DNA (CT-DNA). For promising DNA binding agents, determine the mode of interaction and site specificity of the Pt(IV)-DNA interaction.
- c) Determine the effects of these molecules on prokaryotic and eukaryotic cells using bacterial and cell culture assays to assess cytotoxic effects of the molecules.
- d) Identify trends in behavior of analogous octahedrally-coordinated complexes of the type $M(N-N)_3$ to better predict DNA interaction of these complexes by comparing and contrasting our findings with those published in the literature.

Specifically, this thesis research has focused on the synthesis, characterization, and DNA binding studies of new Pt(IV) molecules. In particular, the first half of this thesis research was spent synthesizing and purifying homoleptic Pt(IV) molecules with 4,7-dimethylphenanthroline (4,7-DMP) and 2,2'-dipyridyl (dipy). The second objective was to characterize this product by Infrared spectroscopy (IR), elemental microanalysis, and X-ray crystallography. The second half of this thesis work focused on developing methods for gel electrophoresis and UV-Vis spectrophotometry using existing ruthenium compounds ($Ru(phen)_3^{+2}$ and $Ru(dipy)_3^{+2}$) which could then be applied to new Pt(IV) compounds.

the valence electrons inward. Platinum(IV) has a high charge density because the +4 charge is located in a dense nuclear core whereas with platinum(II), only a +2 charge is accommodated in the nucleus.

SECTION 2: PROJECT HISTORY

Section 2.1: Synthesis

Since January 1994, when this project was begun, the synthesis and characterization of new Pt(IV) complexes has been one of the primary foci. The bidentate ligands that have been studied include: 1,10-phenanthroline (phen); 2,2'-dipyridyl (dipy); di-2-pyridyl ketone (DPK); 4,7-dimethyl-1,10-phenanthroline (4,7-DMP); and 2,9-dimethyl-1,10-phenanthroline (2,9-DMP). Ligand structures are shown in figure 1.1. Six new Pt(IV) complexes have been synthesized and characterized^{xiii}: tetrachloro-1,10-phenanthrolineplatinum(IV) [Pt(phen)Cl₄]; trichloro-di-2-pyridylketalplatinum(IV) [Pt(DPK)Cl₃] (figure 2.1); dichloro-di-2-pyridylketone-1,10-phenanthrolineplatinum(IV) chloride [Pt(phen)(DPK)Cl₂]Cl₂ (**1**); tetra(hexafluorophospho)-tris(1,10-phenanthroline)platinum(IV) [Pt(phen)₃](PF₆)₄ (**2**); tetra(hexafluorophospho)-tris(4,7-dimethyl-1,10-phenanthroline)platinum(IV) [Pt(DMP)₃](PF₆)₄ (**3**); and tetra(hexafluorophospho)-tris(2,2'-dipyridyl)platinum(IV) [Pt(dipy)₃](PF₆)₄ (**4**) (figure 2.2).

The major obstacle encountered in both the synthesis and the characterization of new Pt(IV) molecules has been the solubility of the complexes. Ideally, water soluble complexes are desired for DNA binding studies so that DNA binding studies may be performed under physiological conditions. During the summer of 1996, a water "friendly" synthesis path (scheme 1) was developed (figure 4.1). Scheme 1 has been used to synthesize what is believed to be a tris-substituted 1,10-phenanthroline complex with Pt(IV) as the center in a complex analogous to the M(N-N)₃ complexes encountered in the literature. The 1996 fall semester was spent expanding this synthetic scheme to homoleptic Pt(IV) centered complexes with different N-N type ligands, particularly 4,7-DMP and dipy.

Purification techniques have been developed for the new compounds synthesized from scheme 1. These techniques stem from the fact that the hexafluorophosphate salts of the Pt(IV)

^{xiii} Not all of these compounds have been fully characterized. Those that are numbered have only been partially characterized. Products from which a crystal structure was obtained in addition to IR, NMR, and elemental analysis are considered fully characterized. These compounds are referred to by name rather than by number.

complexes yielded from scheme 1 are highly soluble in acetone, acetonitrile, and somewhat soluble in methylene chloride. The “raw” product is subjected to one of these solvents, and the desired hexafluorophosphate Pt(IV) salts dissolve readily while the undesired side products favor the solid state. The desired product can then be precipitated with ether.

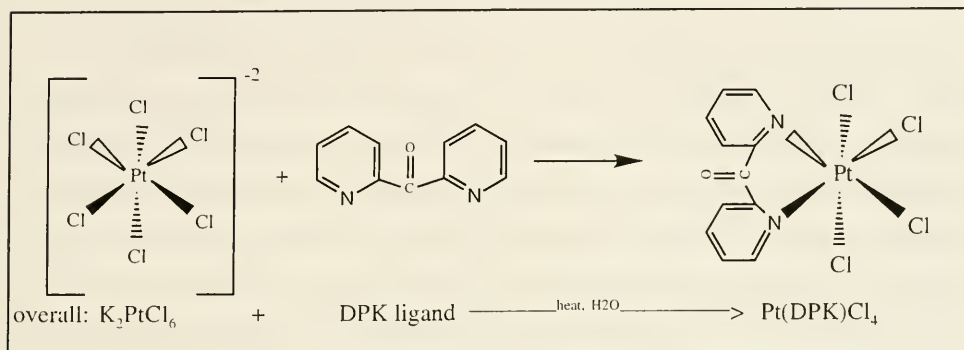


Figure 2.1. Reaction for the synthesis of $Pt(DPK)Cl_4$ (see Results section for characterization data).

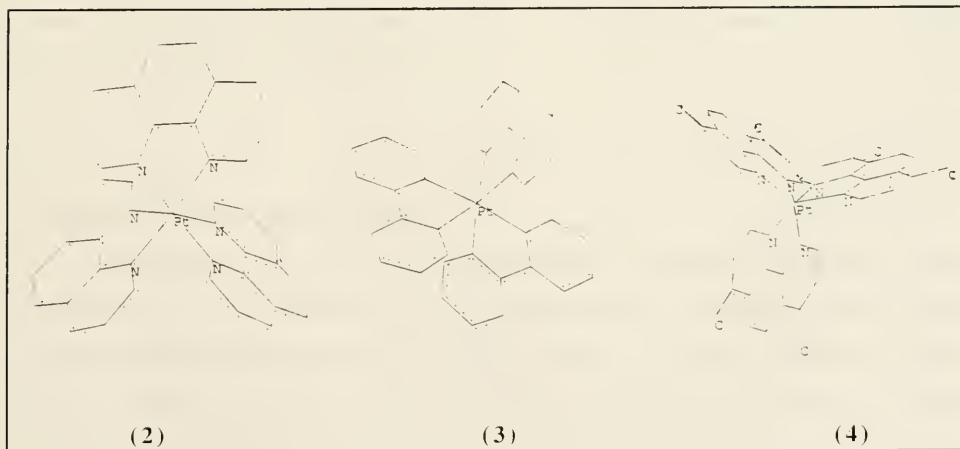


Figure 2.2. Proposed structures of $Pt(N-N)_3^{+4}$ compounds studied in this project: $Pt(phen)_3^{+4}$ (2); $Pt(dipy)_3^{+4}$ (3); and $Pt(4,7-DMP)_3^{+4}$ (4).

Section 2.2: Characterization

The success of a proposed set of reactions in a synthesis is tested by characterization of the products. Methods of analysis include IR spectroscopy, NMR spectroscopy, elemental microanalysis and X-ray crystallography. Prior to subjecting new compounds to characterization techniques it is important to purify the products.

IR spectroscopy and NMR spectroscopy provide a “fingerprint” of the molecule. IR spectroscopy gives information concerning the vibrational interactions of bonds. NMR spectroscopy provides information concerning the coupling of nuclei in molecules. Absorbances in the IR and NMR spectra are characteristic for types of bond interactions, and the combination of peaks is characteristic for molecules. Elemental microanalysis determines the percent composition of the elements present in a sample. The percent compositions found are compared to theoretical percent compositions based on calculations with the proposed sample. To be considered pure, a sample must have its theoretical and found percent compositions within $\pm 0.3\%$ (Fornefeld). For this project, the purified product is sent to Midwest MicroLabs in Indiana for analysis. X-ray crystallography takes a “snapshot” of the sample product by analysis of electron diffraction patterns when an X-ray beam irradiates the sample. A crystal of the product is sent to Dr. Phil Fanwick of Purdue University for analysis.

Section 2.3: DNA Binding Studies

A second major focus has been the development of a strategy for monitoring binding characteristics of the synthesized probes by gel electrophoresis. Ru(phen)_3^{+2} was used with pBR322 to reproduce the experiments of Pyle et al. (1989) as well as those of Kelly et al. (1985) in order to develop a strategy for DNA binding studies which could be applied to the newly synthesized Pt(IV) complexes. Gel electrophoresis studies were done on compound (2) and will continue on compounds (3) and (4) and other M(N-N)_3 complexes as they are synthesized by scheme 1.

Plasmids are circular DNA structures that are normally wound to form supercoiled DNA of a certain writhe. When intercalating agents, restriction enzymes, or "special" enzymes (e.g., topo I and II) interact with the plasmid DNA, the topology is modified, resulting in more dense supercoils, more relaxed supercoils, relaxed circular DNA, or linear DNA, depending upon the interaction. The metal complexes are hypothesized to partially intercalate into the base pairs or to groove bind to the DNA, resulting in partial unwinding of the DNA at the site of interaction. Thus, as the metal complex binds to the plasmid DNA, the supercoiled structure of the plasmid relaxes to a varying degree depending upon the molecular probe composition. In other words, it would be expected that different metal centers as well as different ligands would affect the DNA structure in different ways. For example, ethidium bromide, the classic intercalator, unwinds the DNA by 24° while other known intercalators such as daunomycin and actinomycin unwind the DNA to a lesser extent (Chaires & Suh, 1995; Chaires, 1986; Wang 1974; and Waring 1970).

The mobility of DNA is determined using gel electrophoresis. Both size and shape affect mobility as the smaller fragments can "worm" their way through the crosslinked gel faster than bigger fragments. A closed circular supercoiled DNA plasmid travels faster than relaxed DNA since the supercoiled DNA is more compact than the relaxed DNA. When uncoiled, a supercoiled plasmid DNA such as pBR322 migrates slower due to its increased effective molecular size (i.e., the unwound plasmid seems bigger than the supercoiled plasmid). Since supercoiled DNA is more compact than less supercoiled (more relaxed) DNA, it would be expected that as the plasmid was unwound by the metal complex, the pBR322 bands would migrate slower in the gel. (By way of illustration, if you take a rubber band and twist it until it is tightly wound, it would represent a supercoiled plasmid. Now gradually relax it; this is progressively more relaxed plasmid. The tightly wound form of the rubber band would fit better in a small hole than the unwound rubber band. The "hole" is representative of the pores caused by crosslinking in the gel.) Thus, it would be expected that pBR322 would migrate more slowly on an electrophoretic gel in the presence of a metal complex compared to in its absence.

SECTION 3: CHEMICALS AND EQUIPMENT

Chemicals

The ligands and starting materials: 1,10-phenanthroline; 4,7-dimethyl 1,10-phenanthroline; 2,2'-dipyridyl; potassium hexachloroplatinate(IV); potassium hexafluorophosphate; and citric acid, trisilver salt hydrate were purchased from Aldrich Chemical Company. Bacteriophage lambda DNA Hind III digest and pBR322 DNA were purchased from New England Biolabs. Calf thymus DNA, type VI-A: high gelling temperature agarose, ethidium bromide tris[hydroxymethyl]aminomethane (Trizma base), and disodium ethylenediaminetetraacetic acid (EDTA) were purchased from Sigma. Finally, topoisomerase I (topo I) was purchased from Life Technologies, Gibco.

Equipment

Hewlett Packard 8452A Photodiode Array Spectrophotometer
matched pair of quartz cuvettes, 10 mm path length, Starna Cells, Inc.

Matteson Instruments 4020 Galaxy Series FT-IR

electrophoresis unit, Sigma-Aldrich Techware

Bio-Rad Model 1000/ 500 Power Supply

Bio-Rad Power Pac 1000

pH meter, Orion Research Model 601A/ Digital Ionanalyzer

Fotodyne Foto-Prep I UV Transilluminator

microscope, American Optical Instrument Company

Branson 1210 sonicator

Mettler AE 100 analytical balance

Modulab ModuPure Plus Reagent Grade Water System

SECTION 4: EXPERIMENTAL

Section 4.1: Synthesis

A total of three syntheses were carried out during the fall 1996 semester following the water synthesis scheme (scheme 1, figure 4.1). Synthesis of homoleptic Pt(IV) compounds proceeded using 4,7-dimethyl 1,10-phenanthroline (DMP) and 2,2'-dipyridyl (dipy) in separate syntheses. In synthesis #1 and #2, (N-N) = DMP and in synthesis #3 (N-N) = dipy. The goal of syntheses #1 and 2 was to produce $[\text{Pt}(4,7\text{-DMP})_3](\text{PF}_6)_4$, referred to as compound (**3**). The goal of synthesis #3 was to produce $[\text{Pt}(\text{dipy})_3](\text{PF}_6)_4$, referred to as compound (**4**).

Scheme 1

Distilled/deionized water was used throughout the experiments. Following scheme 1: K_2PtCl_6 (0.2 mmol) was dissolved in a minimum amount of water in a round bottom flask. A two fold excess (6:1 molar ratio of ligand: K_2PtCl_6) of the N-N ligand was then added to the K_2PtCl_6 solution while heating and stirring. Water was added as necessary to aid in solvation and stirred for no longer than 30 minutes. Meanwhile, $\text{Ag}_3(\text{citrate})$ (0.1 mmol) was dispersed in approximately 5 mL of water using the sonicator. This was then added to the K_2PtCl_6 /ligand solution and refluxed for approximately 30 minutes. The solution was then filtered hot on a frit to remove the AgCl solid. The filtrate, a small amount of ligand, and a two fold excess of KPF_6 (8:1 molar ratio of KPF_6 : K_2PtCl_6) were then added to a clean flask. This solution was refluxed approximately 60 minutes and filtered. If any red solid was visible, it was washed with methylene chloride or acetone and reprecipitated with ether. The tan solid left in the frit was then placed in a clean flask with ~50 mL water, a small amount of ligand, and a two fold excess of KPF_6 . This was again refluxed for approximately 60 minutes and filtered. The process was repeated until all of the tan product was converted to red product.

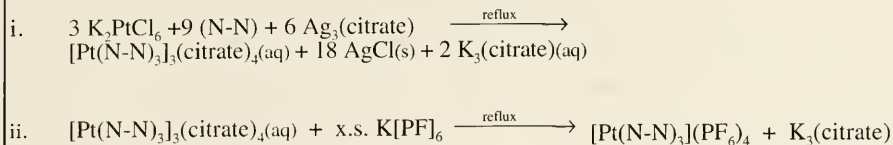


Figure 4.1. Scheme 1: Specific reactions for the synthesis of homoleptic $\text{Pt}(\text{N-N})_3$ complexes.

Purification

Purification techniques were developed for the new compounds synthesized by scheme 1. These techniques stem from the fact that the hexafluorophosphate salts of the $\text{Pt}(\text{IV})$ complexes yielded from scheme 1 are highly soluble in acetone, acetonitrile, and somewhat soluble in methylene chloride and water. Crystalline product was obtained using methylene chloride/ether (synthesis #1) or acetone/ether (synthesis #2 and #3). In all syntheses, both red and beige crystals formed. To further purify the crystalline products, a light microscope and a needle could be used to physically pull apart the two different products. Alternatively, it was found that the red product was highly soluble in acetone while the beige product was only slightly soluble in acetone. To recrystallize the product, acetone was added to the solid product. The red filtrate was collected and recrystallized in acetone/ether. This recrystallization process was repeated for a practical limit of 2-4 iterations (until almost all crystals were red). Further iterations would have resulted in significant loss of the desired sample. Slow diffusion crystal growth systems were set up by dissolving the sample in a solvent in which it was soluble in a small vial and then placing the vial in a jar full of ether, in which the sample is insoluble. The ether vapors that diffuse into the vial with the dissolved sample cause the sample to precipitate. The crystal growth systems were placed in the cold room to slow down the process of crystallization from a few hours at room temperature to a couple of days in the cold room in order to allow for more stable interactions. By decreasing the temperature, the kinetic interactions of the molecules in the system (sample and solvents) are also decreased so that only the most favorable bonds are formed, resulting in pure crystals.

In synthesis #1, the product (**3**) was purified as described above using methylene chloride/ether for the first recrystallization and using acetone/ether subsequently since the product was found to be more soluble in acetone. Crystals of (**3**) were grown following this procedure. Since the crystals were found to decompose when they were dried, crystals of (**3**) were sent "wet" (in a vial with acetone/ether) for X-ray diffraction analysis.

Because of the instability of these crystals to air, another crystal system with DMSO/ ether was used. The products from all syntheses was soluble in DMSO but not in ether, so the ether vapors were used to slowly precipitate the product. The products were subjected to slow diffusion (approximately 4 months) in DMSO/ether in the 4 °C cold room. Crystals of (**3**) were also grown with this system and sent for X-ray diffraction analysis. No crystals of (**4**) were grown.

Section 4.2: DNA Binding Studies - Gel Electrophoresis

Specific objectives for the gel electrophoresis trials are detailed in the following sections. Unless otherwise stated, the information concerning buffers, solutions of metal complexes, and solutions of DNA applies to all gel electrophoresis experiments. Sterile technique was used throughout.

Buffers

Buffers 1, 2, and 3, variations of 50 mM Tris-acetate buffer (TAE), were made as described in table 4.1. A 50x concentration of Buffer 1 (B1) was initially made and then diluted 1: 49 concentrate: water for a final concentration of 50 mM. Buffers 2 and 3 were made from B1 and all were then autoclaved.

Table 4.1: Buffers

Buffer 1 (B1)	50x	48.4 g Tris base 11.42 g glacial acetic acid 20 mL 0.5 M EDTA
Buffer 2 (B2)	1x	B1 + 18 mM NaCl pH 7.0
Buffer 3 (B3)	1x	B2 + 0.94 μ M compound (2)

Metal Complex Solutions

This experiment was developed with ruthenium(II) and platinum(IV) centered $M(N-N)_3$ complexes to compare DNA binding effects (i.e., Does the $Ru(phen)_3^{+2}$ show a different effect than $Ru(dipy)_3^{+2}$ and are these effects also different from compounds (2), (3), and (4)?). Stock solutions of compound (2) and $Ru(phen)_3^{+2}$ were made as given in table 4.2. The solutions were diluted in B2. 0.94 μ M of compound (2) was used^{xiv}. The concentration of compound (2) used in this experiment was verified by UV-Vis spectroscopy according to Beer's Law:

$$c = A_{268} / l \epsilon_{268}$$

where c is the concentration, A_{268} is the absorbance at 268 nm, ϵ_{268} is the absorptivity coefficient ($\epsilon_{268} = 2.871 \times 10^5 \text{ M}^{-1}\text{cm}^{-1}$)^{xv}, and l is the path length = 1 cm.

^{xiv} 9.4 μ M of compound (2) was intended, but 0.94 μ M of the complex was used due to a dilution error.

^{xv} Determined by Dr. Robert Granger, Virginia Military Institute

Table 4.2: Stock Solutions of Metal Complexes

complex	MW	concentration	# grams	total volume with B2
$\text{Ru(phen)}_3\text{Cl}_2$	712.61 g/mol	940 μM (100x)	67 mg	100 mL
$\text{Ru(dipy)}_3\text{Cl}_2$	748.63 g/mol	940 μM (100x)	70 mg	100 mL
$[\text{Pt(phen)}_3](\text{PF}_6)_4$ (2)	1314.00 g/mol	94 μM (10x)	3.1 mg	25 mL
$[\text{Pt(DMP)}_3](\text{PF}_6)_4$ (3)	1399.17 g/mol	94 μM (10x)	3.3 mg	25 mL
$[\text{Pt(dipy)}_3](\text{PF}_6)_4$ (4)	1243.50 g/mol	94 μM (10x)	2.9 mg	25 mL

DNA Solutions

Solutions of bacteriophage lambda DNA digested with Hind III (λ Hind III) and pBR322 were made for electrophoresis according to table 4.3 below.

Table 4.3: DNA Solutions

Stock Solution	Working Solution	Composition
500 $\mu\text{g/mL}$ λ Hind III	0.125 $\mu\text{g/mL}$	5 μL stock λ Hind III + 20 μL B3
1000 $\mu\text{g/mL}$ pBR322	32.4 $\mu\text{g/mL}$ ^{xvi}	3.24 μL stock pBR322 + 96.76 μL B3

Section 4.2A: Gel electrophoresis comparison of (**2**) vs. control

Two 1% agarose gels were made to compare the migration of lambda Hind III and pBR322 in the presence and absence of compound (**2**). The control gel had no complex added (made with B2), and the test gel had 0.94 μM compound (**2**) (made with B3). The wells were loaded as described in table 4.4. The loading buffer (LB) consisted of 0.25% xylene cyanol, 0.25% bromophenyl blue, and 30% glycerin.

^{xvi} This is 100 mM nucleotides. Refer to Appendix B for calculations.

Table 4.4: Composition of Gel Wells

well #	1, 3, 7, 9, 10	2, 8	4, 5, 6
LB	3 μ L	3 μ L	3 μ L
B2 (control) or B3 (Pt complex)	7 μ L	2 μ L	2 μ L
λ Hind III	0 μ L	5 μ L	0 μ L
pBR322	0 μ L	0 μ L	5 μ L

The gels were electrophoresed simultaneously on the same power supply for 2 hours at 50 volts followed by 2 additional hours at 60 volts. The voltage was increased to speed the rate of migration. The gels were then stained with 0.5 μ g/mL ethidium bromide solution for approximately 40 minutes and destained in 1 mM MgSO_4 for an hour at room temperature. The bands were detected with a UV light source and photographed (Polaroid 667 film, f 4.5, 1 second exposure, 30 second development). Since the gels appeared dark, they were restained in ethidium bromide overnight, destained in MgSO_4 for 2 hours, and photographed again (figure 5.5). The band migrations were measured (table 5.2).

Section 4.2B: Gel electrophoresis comparison of $\text{Ru}(\text{phen})_3^{+2}$ vs. $\text{Ru}(\text{dipy})_3^{+2}$ and of $\text{Ru}(\text{phen})_3^{+2}$ vs. (2)

To compare DNA binding with different metal centers (ruthenium(II) and platinum(IV)) and different ligands (phenanthroline and dipyrldyl), four gels were run following the conditions described above. Gel A was the control and had no added metal complex; gel B had 0.94 μ M $\text{Ru}(\text{dipy})_3^{+2}$; gel C had 0.94 μ M $\text{Ru}(\text{phen})_3^{+2}$; and gel D had 0.94 μ M compound (2). Samples loaded in the middle wells were all composed of the same amounts of pBR322 and buffers; likewise, all samples loaded in lanes 2 and 8 were composed of the same amounts of λ Hind III and buffers so that direct comparisons could be made (table 4.4). The gels were electrophoresed simultaneously with the same power supply at 40 volts for 4.5 hours, stained in ethidium bromide overnight, destained approximately 45 minutes in 1 mM MgSO_4 and photographed.

Section 4.2C: Gel electrophoresis as a method for topoisomerase I assay

A topoisomerase I (topo I) assay is being developed to compare the migration of supercoiled pBR322 (control) with pBR322 exhibiting varying degrees of superhelicity due to the presence of DNA binding probes. To assess the migration of totally relaxed pBR322, a topo I assay is being developed following method of Pyle et al.(1989) and Kelly et al.(1985). To determine a method for this assay, Ru(dipy)_3^{+2} and Ru(phen)_3^{+2} were used. Table 4.5 provides some experimental details. The buffers used in the assays are given in table 4.6.

Since the function of topo I is to nick single strands of the plasmid and thus change the topology of the DNA, another consideration of this assay was to determine where the pBR322 would migrate if nicked. The restriction enzyme Bam HI has only one recognition site on the pBR322, thus only one cut in the double stranded DNA is made resulting in one fragment of the same molecular weight as circular pBR322 but with different topology. Bam HI was used to cleave the plasmid, resulting in the linear form of pBR322. A linear sample of pBR322 was run to compare to the supercoiled and relaxed forms of pBR322. 16.5 μL sterile water, 2.0 μL 10x Bam HI buffer (500 mM Tris-HCl, pH 8.0, 100 mM MgCl_2 , 10 M NaCl), 0.5 μg pBR322, and 1.0 μL Bam HI (20 units) were added to a sample tube for linearization.

0.47 to 0.5 μg of pBR322 DNA, 0 to 3 units of topo I, and 0 to 10 μM ruthenium complex were used in each 50 μL reaction mixture. All of the sample reaction mixtures were incubated at 37 °C for 1 to 4 hours (except the λ Hind III marker). After incubation, the DNA was ethanol precipitated following the method of Maniatis in which 150 μL ethanol (trials included chilled and filtered ethanol) was added to each sample. The DNA was allowed to precipitate at -20 °C for 2 hours to several nights. The samples were then centrifuged at 14,000 rpm for 10 minutes at 0 °C, decanted, washed with 70% ethanol, and recentrifuged at 10,000 rpm for 2-3 minutes. The supernatant was again decanted and the DNA pellet was resuspended in 10 μL running buffer plus 3-4 μL loading buffer.

The samples were electrophoresed on 40 mL non-denaturing 1% agarose gels. The gel wells were loaded (table 4.7) and the gels subjected to electrophoresis at 20-55 volts until the dye

migrated to within approximately 1-2 centimeters from the edge of the gel at the negative side. The most common range was 45-55 volts for 5-6 hours. Following electrophoresis, the gel(s) were stained with ethidium bromide for 1 hour to overnight and destained in 1 mM MgSO₄ for 45 minutes. Gels were viewed under UV light and photographed.

The major source of variation in the different topo I trial runs was the buffer used for enzymatic incubation as well as for gel electrophoresis. First, the buffer recommended by Pyle et al. (1989) (TBI) was used (5 mM Tris-HCl pH 7.2; 50 mM NaCl; 1 mM MgCl₂; 1-10 μ M Ru complex). After a few trials in which no DNA bands were observed, the method was simplified for troubleshooting to samples of only λ Hind III marker and two different concentrations of pBR322. The ethanol precipitation procedure was also tested by subjecting two of the samples to ethanol precipitation while running the analogous samples without ethanol precipitation. None of these "controls" had topo I or Ru complex. After noting that a pH gradient formed in the TBI buffer, gels were electrophoresed at a constant current of 100 mA to reduce chances of decomposition of buffer at high current. When this strategy also did not yield observable bands, other buffers were tried including the standard suggested reaction buffer (BS) for topo I (50 mM Tris-HCl pH 7.5; 50 mM KCl; 10 mM MgCl₂; 0.5 mM DTT; 0.1 mM EDTA; and 30 μ g/mL BSA) and Tris-borate running buffer (TBE) (89 mM Tris base; 89 mM boric acid; 2 mM EDTA). This TBE running buffer seemed to be the most stable and had the advantage that it could be reused for subsequent runs. The gel for each trial was made from the same 1x batch of TBE as the running buffer to ensure that the salt concentrations did not vary. Additionally, ruthenium complexes of interest were tested for the effects of topo I on unwinding under the lowered salt conditions of BL buffer (5 mM Tris-HCl pH 7.5; 5 mM KCl; 0-1.5 mM MgCl₂; 0.5 mM DTT; and 30 μ g/mL BSA). New topo I was also purchased to try to obtain observable bands since it was uncertain whether or not the first batch ordered had been denatured at some point.

Table 4.5: Comparison of Topoisomerase I Assay Methods

assay conditions	Pyle et al.(1989)	Kelly et al.(1985)	Kelly, Murphy (1985)	Garcia
amt. DNA	0.47 µg	0.5 µg	1.6 µg	0.47-0.5 µg
reaction vol.	50 µL	50 µL	50 µL	50 µL
buffer ^{xvii}	TB1	BL	BS	TB1; BS; BL
amt. topo I	2-4 units	not given	not given	1-3 units
incubation	1 hr 37 °C	3 hrs 37 °C	4 hrs 37 °C	1-4 hrs 37 °C
complexes	mixed ligand Ru(II) complexes	Ru(phen) ₃ ⁺² Ru(dipy) ₃ ⁺² 2 other mixed ligand Ru complexes	porphyrins	Ru(phen) ₃ ⁺² Ru(dipy) ₃ ⁺²
DNA treatment	EtOH ppt @ -20 °C resuspend in 20 µL buffer (no Mg ⁺²)	extract complex: make aq. layer to 0.3 M NaAc; EtOH ppt DNA; dry; resuspend in 10 µL TBE	extract porphyrin; make aq. layer to 0.3 M NaAc; EtOH ppt DNA; dry; resuspend in 10 µL TBE	EtOH ppt @ -20 °C; centrifuge; wash with 70% EtOH; centrifuge; resuspend in 10µL TBE

^{xvii} See Table 4.6 for buffer compositions.

Table 4.6: Buffer Compositions for Topoisomerase I Assays

buffer	composition
TBI	5 mM Tris-HCl pH 7.2; 50 mM NaCl; 1 mM MgCl ₂ ; 1-10 μ M Ru complex
BL	5 mM Tris-HCl pH 7.5; 5 mM KCl; 0 - 1.5 mM MgCl ₂ ; 0.5 mM DTT; and 30 μ g/mL BSA
BS	50 mM Tris-HCl pH 7.5; 50 mM KCl; 10 mM MgCl ₂ ; 0.5 mM DTT; 0.1 mM EDTA; and 30 μ g/mL BSA
TB2	0.5% (v/v) glycerol; 0.05 mM DTT; 10 mM Tris-HCl; 0.2 M NaCl; 0.2 mM EDTA
TBE	89 mM Tris base; 89 mM boric acid; 2 mM EDTA

Table 4.7: Composition of Lanes in Topoisomerase I Assays

lane #	1	2	3	4	5-10
well composition	λ Hind III + running buffer (RB)	pBR322 + Bam HI + Bam HI buffer + H ₂ O	pBR322 + RB	pBR322 with topo I	pBR322 with topo I and increasing concentrations of M(N-N) ₃ metal complex
expected DNA form	linear fragments	linear	supercoiled	relaxed	various degrees of relaxation

Section 4.3: DNA Binding Studies - UV-Vis Absorption Spectroscopy

The effect on the absorption spectra of $M(N-N)_3$ metal complexes in the presence of CT-DNA can be determined by obtaining UV-Vis spectra for the metal complexes in 10 mM phosphate buffer (5 mM K_2HPO_4 and 5 mM KH_2PO_4 , pH = 6.9) in the presence and absence of CT-DNA (Kelly et al., 1985). Spectroscopic studies developed for $Ru(phen)_3^{+2}$ by Kelly were repeated in order to develop a similar assay which could be applied to $Pt(IV)$ $M(N-N)_3$ complexes. A matched pair of quartz cuvettes were used in this study. For each cuvette, scheme 2 was followed (figure 4.2). The spectrophotometer was blanked with phosphate buffer and 10 μ M to 20 μ M (depending on the trial number) $Ru(phen)_3^{+2}$ was then added to the cuvette by pipetting 11.5 μ L of stock (~940 μ M) $Ru(phen)_3^{+2}$ to 500 μ L total volume inside the cuvette. The absorbances at 446 nm (A_{446}) and 448 nm (A_{448}) were determined (λ max for $Ru(phen)_3^{+2}$ is 447 nm but the 2 nm resolution limit of the instrument prohibited the determination of A_{447}). To cuvette #1, 10.96 μ L of phosphate buffer was added and the A_{446} and A_{448} were determined. To cuvette #2, 10.96 μ L of 23 mM CT-DNA in phosphate buffer was added to yield a P/D ratio of approximately 40^{xviii}. The P/D ratio allows for a controlled amount of DNA to be added to the metal complex by taking into consideration the molar concentration of phosphates in the DNA compared to the molar concentration of metal complex. The A_{446} and A_{448} were then determined for cuvette 1 in the absence of CT-DNA and cuvette 2 in the presence of CT-DNA.

Calculations

A_{447} was determined by taking the average of A_{446} and A_{448} . The percent change in the $A_{\lambda_{max}}$ was calculated by taking the difference between the absorbances in the absence (A_{abs}) and in the presence (A_{pres}) of CT-DNA, then dividing by the absorbance at lambda max of the sample in the absence of CT-DNA and multiplying by 100%:

^{xviii} Refer to Appendix C for calculations of P/D.

$$\% \Delta A = \frac{A_{\text{abs}} - A_{\text{pres}}}{A_{\text{abs}}} \times 100\%$$

These percent change values were used to determine the extent to which the $\text{M}(\text{N-N})_3$ metal complex interacted with the CT-DNA.

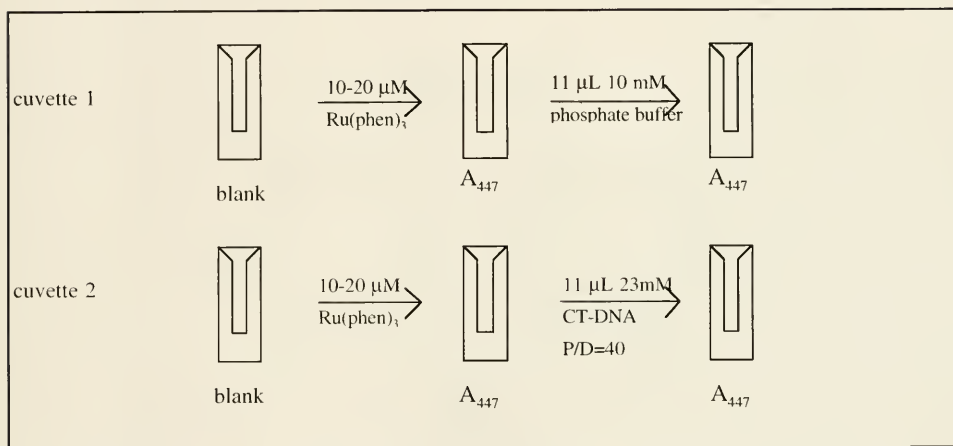


Figure 4.2. Scheme 2: UV-Vis experimental plan. Matching cuvettes were used. 10 mM phosphate buffer was used as the blank. To both cuvettes, the same amount of metal complex was added and the A_{447} was obtained. For cuvette 1, 11 μL additional buffer was added and the A_{447} was again obtained. For cuvette 2, 11 μL of 23 mM CT-DNA was added and the A_{447} was obtained.

SECTION 5: RESULTS AND DISCUSSION

Section 5.1: Synthesis

Synthesis milestones since the project began include the full and partial characterization of Pt(phen)Cl_4 (figure 5.1), Pt(DPK)Cl_3 (figures 5.2, 5.3 and table 5.1) and $[\text{Pt(phen)}_3](\text{PF}_6)_4$ compound (2) (table 5.1 and figure 5.4). Synthesis schemes varied for each product^{xix}.

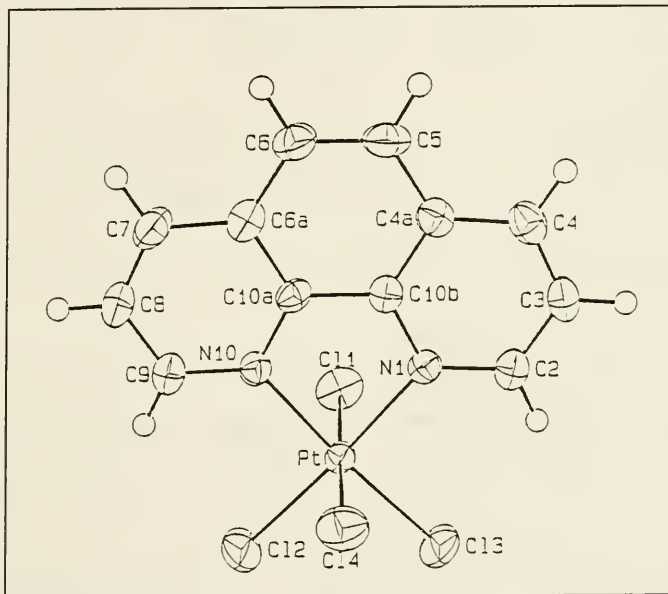


Figure 5.1. X-ray crystal structure of $[\text{Pt(phen)Cl}_4]$. Selected bond lengths and angles: $\text{N}(1)\text{-Pt}$ 2.037 Å; $\text{N}(10)\text{-Pt}$ 2.042 Å; $\text{Cl}(1)\text{-Pt}$ 2.317 Å; $\text{Cl}(2)\text{-Pt}$ 2.302 Å; $\text{Cl}(3)\text{-Pt}$ 2.299 Å; $\text{Cl}(4)\text{-Pt}$ 2.309 Å; $\text{N}(1)\text{-Pt-N}(10)$ 80.6°; $\text{Cl}(2)\text{-Pt-Cl}(3)$ 89.05°; $\text{Cl}(2)\text{-Pt-Cl}(4)$ 91.6°; $\text{Cl}(1)\text{-Pt-Cl}(2)$ 91.6°; $\text{Cl}(1)\text{-Pt-Cl}(3)$ 90.93°; $\text{Cl}(3)\text{-Pt-Cl}(4)$ 91.36°; $\text{N}(1)\text{-Pt-Cl}(3)$ 95.1°; $\text{N}(10)\text{-Pt-Cl}(2)$ 95.3°.

^{xix} The experimental schemes are not included in this thesis since they were not used during the course of the 1996-1997 academic year during which senior thesis research work was done. Results are included to establish that the synthesis of new platinum (IV) $\text{M}(\text{N-N})_x$ compounds is possible (where $x = 1, 2, 3$; mono, bis, or tris substituted, respectively)

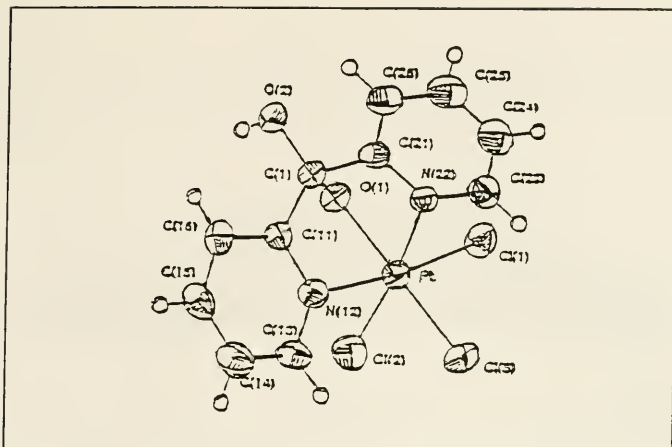


Figure 5.2. X-ray crystal structure of $\text{Pt}(\text{di-2-pyridylketal})\text{Cl}_3$. This is the tautomer of the synthesized $\text{Pt}(\text{di-2-pyridylketone})\text{Cl}_4$ product.

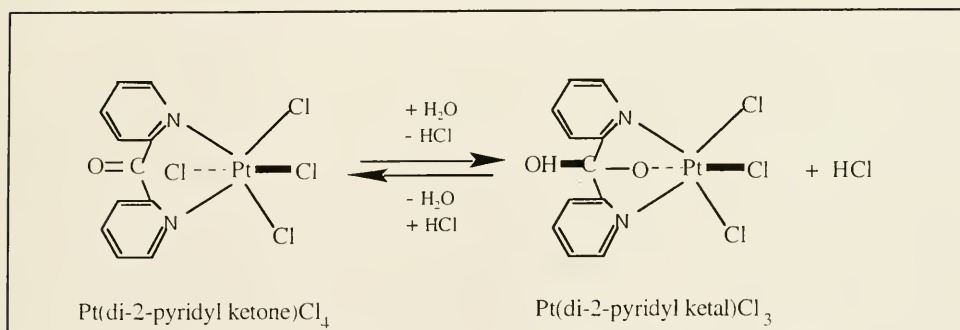


Figure 5.3. Representation of the tautomerization of $\text{Pt}(\text{di-2-pyridyl ketone})\text{Cl}_4$ and $\text{Pt}(\text{di-2-pyridylketal})\text{Cl}_3$.

The crystal structure of $\text{Pt}(\text{DPK})\text{Cl}_4$, a ketone, determined that the compound underwent tautomerization to $\text{Pt}(\text{DPK})\text{Cl}_3$, an enol (figure 5.3). Tautomers are special isomers that are ketones or enols (unsaturated alcohols) (Considine, 1984). In tautomerism, the two isomeric forms of a compound are in equilibrium, each of which exhibits characteristic reactions. Since they are isomers, they have the same elements in the same number, but with different bonds. The

percent compositions of the elements present in each isomer (tautomer) would therefore be the same for each form.

Table 5.1 Microanalysis results
for $\text{Pt}(\text{DPK})\text{Cl}_4$ and $[\text{Pt}(\text{phen})_3][\text{PF}_6]_4$ (compound **(2)**)

Microanalysis	%C	%H	%N	%Pt
$[\text{Pt}(\text{DPK})\text{Cl}_4]$				
Theory	25.35	1.55	5.38	37.44
Found	25.32	1.53	5.37	37.22
$[\text{Pt}(\text{phen})_3][\text{PF}_6]_4$ compound (2)				
Theory	32.87	1.84	6.39	not
Found	32.92	2.04	6.29	obtained

Synthesis experiments conducted during the 1996 fall term followed scheme 1 (figure 4.1). The starting material for the syntheses was K_2PtCl_6 ; this was used to avoid harsh reaction conditions associated with platinum compounds (chelates^{xx}) that have poor leaving groups. In other words, the species associated to the Pt(IV) center (Cl, inner sphere and K, outer sphere) of K_2PtCl_6 dissociate from the center relatively easily under conditions that do not favor their association. The products of the synthesis were visibly impure, as observed by the different colors of crystals that formed (red and beige). Following the purification scheme of repeated crystalline precipitation, most of the product was red with some beige impurity.

The whitish/beige "impurities" may be Pt(II) complexes since Pt(II) complexes are known to be white. Furthermore, it is known that the preferred oxidation state of platinum is +2 rather than +4 so the Pt(IV) could have been easily reduced to Pt(II), resulting in a mixture of both Pt(II) and Pt(IV) products. Another hypothesis is that the impurity may be excess ligand or other starting materials used in excess that have not reacted.

^{xx} A chelate is a complex containing at least one polydentate ligand that forms a ring of atoms including the central metal atom.

Compound (3)

IR spectra of compound (3) produced from different scheme 1 synthesis trials were compared to each other to confirm that the products formed were the same; thus, scheme 1 is reproducible. The IR spectrum of compound (3) was superimposed with the IR spectra of compound (2) and $[\text{Ru}(\text{phen})_3](\text{PF}_6)_2$ for comparison of the major peaks (figure 5.4). The striking similarities suggest analogous compounds.



Figure 5.4. The IR spectrum of compound (3) (bottom) superimposed on the IR spectra of compound (2) (middle) and $[\text{Ru}(\text{phen})_3](\text{PF}_6)_2$ (top) for comparison of the major peaks. The striking similarities suggest analogous compounds.

The red crystals of syntheses #1 and #2, compound (3), grown in acetone/ether were long, hollow, hexagonal, ruby red needle-like rods; some were also branched and fractured and thus did not exhibit a visibly uniform structure. When the crystals were exposed to air, they degraded, becoming very brittle and breaking into small powdery fragments when physically disturbed. The crystals in air could be observed to gradually curl and split. Accordingly, "wet" crystals (in ether)

were sent for X-ray diffraction analysis. According to Dr. Fanwick, they were able to diffract light, but decomposed before he could get them on the slide to be X-rayed. This is because the acetone/ether used for the crystal growth is readily volatile and upon vaporization the bonds are no longer stabilized by the ether. In other words, the ether is not retained in the crystal lattice. Since it is the ether that precipitates the product, the evaporation of ether makes the crystals susceptible to decomposition. The crystals were able to diffract light, suggesting that they should be able to be analyzed. Therefore, another solvent system had to be found that would be retained in the crystal lattice for a longer time. Because DMSO is not especially volatile, new crystals were grown in DMSO/ether. This process took much more time than the acetone/ ether system, likely because DMSO is such a favorable solvent. This may be a result in a difference of phase preference (crystal or solution) for the $M(N-N)_3$ compound that is less pronounced in DMSO/ether than in acetone/ether.

As a result of the DMSO/ether crystal system, large, ruby red, hexagonal, rod-shaped crystals were grown by slow diffusion (4 months) in the cold room. These crystals were more stable to the air than those grown in acetone/ether. Unfortunately, their stability was not adequate enough to withstand exposure to air overnight while awaiting X-ray analysis, and they also decomposed. Thus, a crystal structure has not yet been obtained. However, Dr. Fanwick reported that they did in fact diffract light, a promising consolation since this means a crystal structure is possible under more vigilant handling during analysis. The crystal growing conditions are currently being applied to more of compound (3) and once these are ready for X-ray analysis, Dr. Fanwick will be forewarned about the susceptibility to decomposition.

A sample of synthesis #1 was sent for microanalysis once the product was all red indicating a pure sample, however the percent compositions found for C, H, N, and Pt were out of range for all possible products of synthesis #1, including compound (3) and its mono and bis-substituted intermediates as well as the starting products alone. The results of the microanalysis, therefore, can not be used for characterization of the synthesized complex and are most likely due to side reactions which occurred during the harsh conditions of elemental analysis.

Compound (4)

The crystals formed from synthesis #3, compound (4), were red, tiny, needle-like structures clumped together to resemble "starbursts" and "bowties" under a light microscope. The crystals grown from acetone/ether have not been sent for X-ray analysis because they too would probably exhibit the same decomposition in air as compound (3), and at this point it would be worthwhile to await results of the compound (3) crystals from DMSO/ether to determine whether it is worthwhile to apply this solvent system to this synthesis.

A beige film and some other beige, fibrous co-precipitates formed and covered the glass surface of the vial in which the compound was placed for purification. These co-precipitates are in the process of purification and will be sent for microanalysis. Taking into account the loss of product to impurity and repeated transfers, the syntheses resulted in a small percent yield. Larger scale syntheses are needed for further characterization and DNA binding studies. Thus, the next step is to synthesize compound (3) on a larger scale so that sufficient product may be used for crystal growth as well as DNA binding studies.

Section 5.2: Preliminary DNA Binding Studies - Gel Electrophoresis

Section 5.2A: Gel electrophoresis comparison of (2) vs. control

This gel electrophoresis experiment showed distinct band migration and an observable difference between the control gel and the gel with 0.94 μM compound (2) (figure 5.5). The dilution error encountered proved that even at such low concentrations, a DNA binding effect can be observed for compound (2). The first three bands of the λ Hind III and the first band in pBR322 in both the control gel and the gel with compound (2) (the (2) gel) migrated similar distances. The fourth band in the (2) gel was retarded in comparison to in the control gel. The fifth and sixth bands were retarded distinctly more in the (2) gel compared to the control gel. The first bands of the pBR322 migrated marginally slower in the (2) gel when compared to the control gel, while the third bands of pBR322, which are the most prominent bands, were noticeably

retarded in the (2) gel. The migration difference between the fifth and sixth bands (those most affected) of λ Hind III in the control gel and the (2) gel were compared to the migration difference of the third band of pBR322 (again, this was the most affected and displays a similar overall rate) in the control and in the (2) gel, it was seen that migration retardation effect was approximately the same (13.5%-14.9% change) (table 5.2). In other words, the presence of the metal(N-N)₃ affected the migration of the supercoiled plasmid and the smaller pieces of λ Hind III digest to approximately the same extent.

The relative migration difference of the marker bands and the (2) gel bands was similar. Thus, the mode of interaction of compound (2) with plasmid DNA is uncertain. Although research with analogous M(N-N)₃ compounds by Barton and others in earlier studies (Barton et al., 1982; 1983; 1984; 1986; Friedman et al., 1991; Krotz et al., 1993; Sitlani, et al., 1993) proposed intercalation of the compounds into the DNA, more recent studies (Satyanarayana et al., 1993) prove that this assertion is not fully correct. However, from these results it is known that compound (2) interacts with both lambda and pBR322 DNA. This is evidenced by a retardation of the migration of the DNA bands for both types of DNA in the (2) gel. Indeed, a 13.5% retardation was seen for the most prominent band of pBR322 (3rd band down) compared to the analogous control lane.

$$\% \text{ retardation} = \left(\frac{\text{pBr322}_{(control)} \text{ band migration} - \text{pBr322}_{(2)} \text{ band migration}}{\text{pBr322}_{(control)} \text{ band migration}} \right) \times 100\%$$

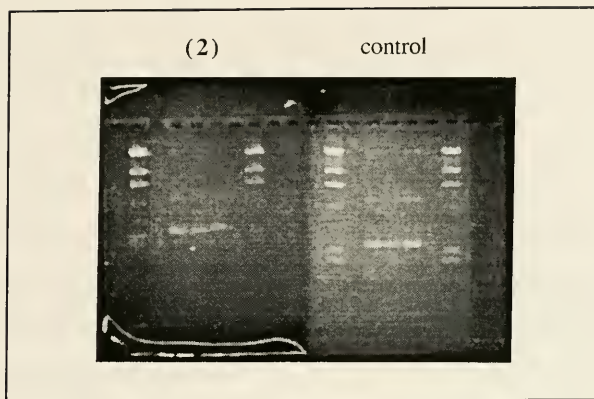


Figure 5.5. The 1% non-denaturing agarose gels above are the (2) gel (0.94 μ M) and the control gel (no metal complex present). The outer lanes are λ Hind III (0.5 μ g) and the inner lanes are pBR322 (0.2 μ g). Migration distances are given in table 5.2

Table 5.2. Migration distances of Lambda Hind III fragments and pBR322 in control and compound (2) gels

MW (bp)	DNA and band #	control distance (mm)	compound (2) distance (mm)	% change
23130	(λ Hind III) 1	4.5	4.3	4.4
9416	(λ Hind III) 2	7.2	7	2.8
6557	(λ Hind III) 3	9.4	8	14.9
4361	(λ Hind III) 4	12.6	12	4.8
2322	(λ Hind III) 5	19.4	16.5	14.9
2027	(λ Hind III) 6	20.7	17.7	14.5
4363	(pBR322) 1	4.5	4.5	0
4363	(pBR322) 2	11.5	11	4.3
4363	(pBR322) 3	18.5	16	13.5

It is also of interest to note that the retardation effects are not due to differences in ionic strength. In order for direct comparisons to be made, the ionic strength of the control buffers and the metal complex buffers must be equivalent. This is a consequence of the effect of ionic strength on gel migration because the ionic strength affects the relative charge of the molecule to be electrophoresed (metal complex) and the voltage of the buffer. This therefore affects migration towards the positive electrode. Any difference in ionic strength depends on salt concentration in the buffer. The ionic strengths of the buffers without metal complex and with metal complex (**2**) were calculated according to the formula:

$$I = \frac{1}{2} \sum_i Z_i^2 c_i \quad \text{for } i = \text{each ion}$$

where I = ionic strength, Z = charge, and c = concentration of ion. The ionic strength of the 18 mM NaCl in the buffer was calculated to be 0.01800 while for 0.94 μ M of the complex in the same buffer was calculated to be 0.0180094 for compound (**2**) (assuming it is [Pt(phen)₃](PF₆)₄ as the characterization data suggest) and 0.01800282 for Ru(phen)₃Cl₂. To make up for this difference, 144 μ g of NaCl in 375 mL of buffer (to fill the electrophoresis unit and to make the gel) would have to be added to the buffer with which the Ru(phen)₃Cl₂ gel was run. The difference in the ionic strengths was thus assumed to be negligible although no experiment was performed to test this assumption.

Section 5.2B: Gel electrophoresis comparison of Ru(phen)₃⁺² vs. Ru(dipy)₃⁺² and of Ru(phen)₃⁺² vs. (**2**)

The gel electrophoresis method described above was applied to four gels simultaneously to assess differences in DNA migration due to two different metal centers and two different ligands. The gels were grouped: A, B, C (figure 5.6); and A, C ,D (figure 5.7) for comparison due to different metal centers (Ru and Pt) and due to different ligands (phen and dipy). Table 5.3 gives migration distances for the 3rd band of pBR322 (supercoiled plasmid) and for the 5th band of λ

Hind III marker DNA (MW 2322 bp) for each of the gels A-D. Gel A was the control and had no complex in it; gel B had $0.94\ \mu\text{M}$ $\text{Ru}(\text{dipy})_3^{+2}$; gel C had $0.94\ \mu\text{M}$ $\text{Ru}(\text{phen})_3^{+2}$; and gel D had $0.94\ \mu\text{M}$ compound (2).

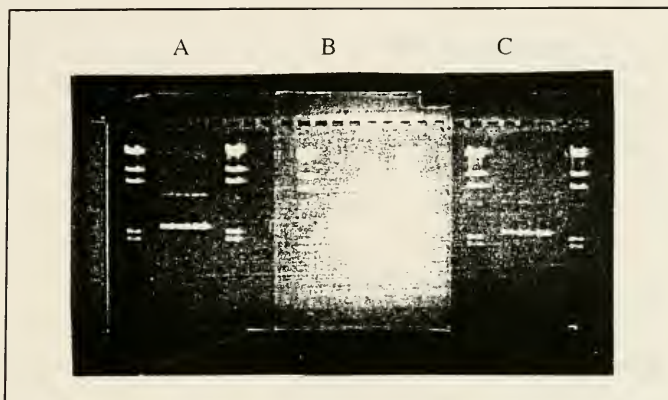


Figure 5.6. 1% non-denaturing agarose gels: control (A), $\text{Ru}(\text{dipy})_3^{+2}$ (B), and $\text{Ru}(\text{phen})_3^{+2}$ (C). Lanes 1, 5: λ Hind III; Lanes 2, 3, 4: pBR322.

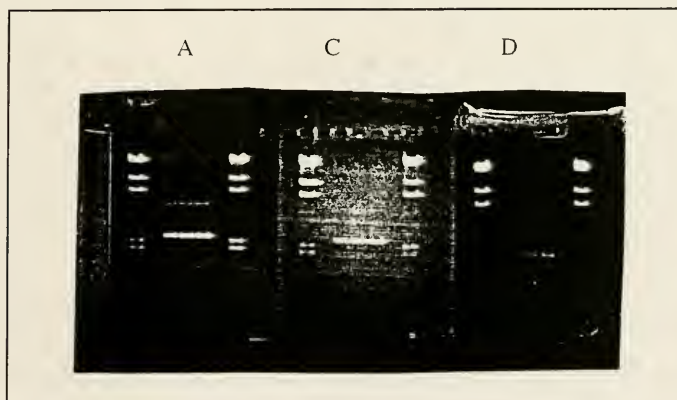


Figure 5.7. 1% non-denaturing agarose gels: control (A), $\text{Ru}(\text{phen})_3^{+2}$ (C), and compound (2) (D). Lanes 1, 5: λ Hind III; Lanes 2, 3, 4: pBR322.

Table 5.3. Migration distances and percent change of the 5th fragment of Lambda Hind III and the 3rd band of pBR322 in A: control, B: Ru(dipy)₃⁺², C: Ru(phen)₃⁺², and D: (2) complex gels.

gel (distance migrated in mm)	5th band λ Hind III MW marker 2322 bp	3rd band pBR322
A	18	17.5
B	20.5	20
C	19.5	18.5
D	22.5	22
% change		
A vs. B	12.2%	12.5%
C vs. B	4.9%	7.5%
A vs. C	7.7%	5.3%
A vs. D	20%	18.2%
C vs. D	13.3%	13.6%

Retardation of pBR322 DNA migration was expected in the presence of the metal complexes, with the amount of retardation depending upon the metal center and the ligand involved. Ru(phen)₃⁺² was expected to retard the migration of DNA more than Ru(dipy)₃⁺² since Ru(phen)₃⁺² has been shown to unwind DNA almost as much as the classic intercalator ethidium bromide (Kelly et al., 1985). However, for both comparison groups (A, B, C and A, C, D), a retardation in the control DNA (both pBR322 and λ Hind III instead of just for pBR322) was observed. Table 5.3 gives the percent change of the DNA in the control gel compared to the DNA in the presence of M(N-N)₃ complexes. The complexes were observed to enhance migration rather than retard it as expected. Accordingly, compound (2) enhanced migration of pBR322 the most, followed by Ru(dipy)₃⁺² and then Ru(phen)₃⁺². This could mean that the plasmid DNA is being wound tighter, but this should have no effect on the topology of the linear DNA since it is not

supercoiled. The fact that the DNA in the control gel migrated slower compared to the DNA in the presence of the $M(N-N)_3$ complexes could indicate that the conditions were not precisely the same for all four gels even though all gels were made with 40 mL buffer and 0.4 g agarose. For example, the running buffer was poured over the gels until they were covered but the volume was not measured. This could have an effect on the current through the electrophoresis unit resulting in differing migration rates of the DNA in each gel. This experiment should be repeated with an exact buffer volume. Also, the migration of the bromophenol blue dye present in the LB should be monitored to determine if any effects observed are due to the interaction of the $M(N-N)_3$ complexes. Under identical conditions, the migration of the dye should not be affected.

Section 5.2C: Gel electrophoresis as a method for topoisomerase I assay

The first buffer used (TB1) proved difficult to work with, evidenced by the pH gradient that formed during electrophoresis (basic at negative electrode and acidic at positive electrode). This gel was run at constant voltage of 50 volts and the current rose to approximately 300 mA causing the buffer to decompose. Under more favorable conditions, the current remains near 100 mA, and the voltage near 20 volts. No bands could be seen during this experiment which suggested degradation of the DNA by acidic condition.

Another gel was run with TBE and BS buffers and samples containing topo I and decreasing concentrations of $Ru(dipy)_3^{+2}$. These conditions yielded observable bands (figure 5.8); however, no significant differences in the relaxed form of pBR322 (with topo I, lane 4) versus the supercoiled form of pBR322 (lane 3) were seen. Additionally, no effects were seen for pBR322 in the presence of $M(N-N)_3$ complex and topo I (lanes 5-10).

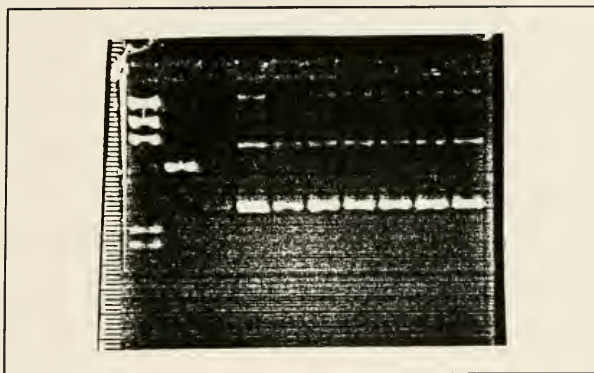


Figure 5.8. Topoisomerase I assay. 1% non-denaturing agarose gel with TBE running buffer and standard topo I reaction buffer; lane 1 = λ Hind III; lane 2 = pBR322 + Bam HI (linear pBR322); lane 3 = pBR322; lane 4 = pBR322 + 1 unit topo I; lanes 5-10 = pBR322 + 1 unit topo I + decreasing concentrations of Ru(dipy)_3^{+2} ($\sim 10 \mu\text{M}$ - $\sim 2 \mu\text{M}$).

The topo I assay was repeated with Ru(phen)_3^{+2} and new sample of topo I enzyme, TBE and BS buffers. The samples were treated as described in the experimental section and very faint, indistinct bands could be seen in this gel (figure thus not included).

The Mg^{+2} concentration affects the intercalation of certain compounds. Thus, Ru(phen)_3^{+2} and Ru(dipy)_3^{+2} complexes have been tested for the effect of topo I on unwinding under low salt concentrations (BL buffer). Magnesium ion concentration (0.0-1.5 mM MgCl_2) has been shown to have an effect on the interaction of Ru(phen)_3^{+2} with DNA. In fact, Kelly et al. (1985) determined that maximum unwinding occurred in the absence of Mg^{+2} . Therefore, the Mg^{+2} concentration was varied in some of the experiments.

Because no detectable shift in the migration of pBR322 in the presence of topo I was seen with the addition of Ru(phen)_3^{+2} when using the standard reaction buffer (BS), a low salt buffer (BL) was used in which the concentrations of Tris-HCl, KCl, and MgCl_2 were decreased 10 fold and no EDTA was added compared to the BS (table 4.6). The concentration of Ru(phen)_3^{+2} was

varied from 1 to 10 μM ; 0 and 1.5 mM MgCl_2 were used in the reaction.

One set of samples was incubated in BL ($[\text{Mg}^{+2}] = 0 \text{ mM}$) and the other set in BL ($[\text{Mg}^{+2}] = 1.5 \text{ mM}$) for 3 hours at 37 °C. A distinct 6 band ladder was seen for lambda Hind III; a large, bright band was observed for linearized pBR322 with Bam HI; no bands were seen for the samples incubated in BL ($[\text{Mg}^{+2}] = 0 \text{ mM}$); and two light bands and one heavy band for each sample were seen for samples incubated in BL ($[\text{Mg}^{+2}] = 1.5 \text{ mM}$) (figure 5.9). No apparent differences in migration due to topo I or to $\text{Ru}(\text{phen})_3^{+2}$ were observed. However, a more thorough analysis of the results is needed. Other possible methods are described by Wang (1974) and Waring (1970). However, instrumental and time constraints were limiting factors for further analysis.

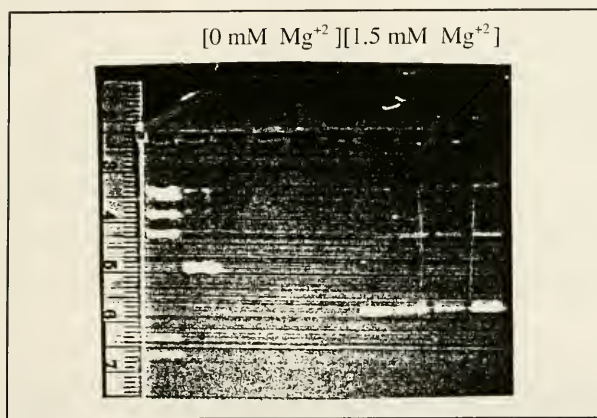


Figure 5.9. Gel electrophoresis of pBR322 in the absence and presence of topo I and $\text{Ru}(\text{phen})_3^{+2}$ with two different reaction buffers varying in $[\text{Mg}^{+2}]$. Lane 1 = λ Hind III; lane 2 = pBR322 linearized by Bam HI; lane 3 = pBR322; lane 4 = pBR322 plus topo I (2 units); lane 5 = pBR322 plus topo I (2 units) and 1 μM $\text{Ru}(\text{phen})_3^{+2}$; lane 6 = pBR322 plus topo I and 10 μM $\text{Ru}(\text{phen})_3^{+2}$ in BL ($[\text{Mg}^{+2}] = 0 \text{ mM}$); lanes 7-10 = same as 3-6 but in BL ($[\text{Mg}^{+2}] = 1.5 \text{ mM}$).

Although the method was improved and bands were observed, the results of this topo I assay are not conclusive since no distinction in the expected migration for pBR322 in the absence (supercoiled) and presence (relaxed) of topo I could be seen. Based the known function of topo I (nicking/ cleaving enzyme) it would be expected that the pBR322 in the absence of topo I should migrate noticeably faster than pBR322 in the presence of topo I. This effect was not observed for any of these trials. The reason for this is uncertain. Possible explanations may include: 1.) insufficient incubation time or 2.) insufficient amount of topo I in the reaction. These were addressed by the method of Kellher (1975) by increasing the topo I to 2 units per reaction and increasing the incubation time to 25 hours without testing for metal complex effects and electrophoresing as before. Again, no observable distinction was observed between supercoiled pBR322 and “relaxed” pBR322.

SECTION 5.3: Preliminary DNA Binding Studies- UV-Vis Absorption Spectroscopy

UV-Vis results and discussion with Ru(phen)_3^{+2} and CT-DNA

In this experiment, the absorption spectra of $10\mu\text{M}$ - $15\mu\text{M}$ Ru(phen)_3^{+2} had an absorbance of approximately 0.2 to 0.3 at the λ max (447 nm) (table 5.4 and figures 5.10, 5.11).

Table 5.4 Changes in A_{447} Ru(phen)_3^{+2}

run-cuvette	A_{447}	% ΔA_{447} = (A-B)/A * 100%	effective % ΔA_{447} with CT-DNA
A-1	0.2354355		
B-1	0.2170715	7.800	
			6.191
A-2	0.2555845		
C-2	0.2198255	13.991	

Table 5.4. A= buffer + 11.5 μL Ru(phen)_3^{+2} ; B= A + 10.96 μL buffer; C= A + 10.96 μL 23 mM CT-DNA (P/D ~ 40). Kelly et al. (1985) showed UV-Vis spectra of CT-DNA in the presence and absence of Ru(phen)_3^{+2} to have A_{447} of approximately 0.22 and 0.20, respectively.

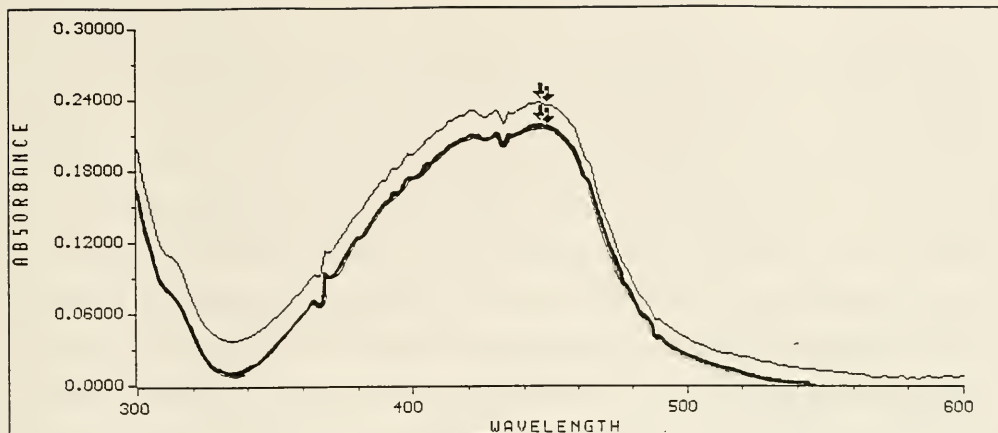


Figure 5.10. UV-Vis Absorption spectra of $\text{Ru}(\text{phen})_3^{+2}$ in the absence of CT-DNA. The top spectrum is with 500 μL total volume, concentration approximately 12.4 μM . The bottom spectrum is with 511 μL total volume, concentration approximately 11.4 μM . A 7.8% change in the A_{447} is observed for concentration changes.

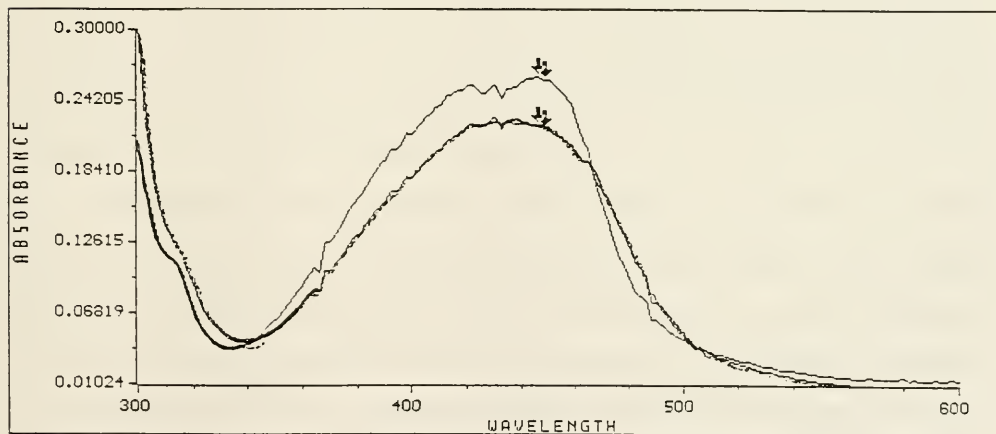


Figure 5.11. UV-Vis Absorption spectra for $\text{Ru}(\text{phen})_3^{+2}$ in the absence and presence of CT-DNA. The top spectrum is in the absence of CT-DNA with 500 μL total volume. The bottom spectrum is in the presence of CT-DNA with 511 μL total volume. A total change of 14.0% in the A_{447} is observed for concentration changes and CT-DNA binding effects. Based on the results shown in figure 5.10 above, a 7.8% change is accounted for by change in concentration; thus a 6.2% change in the A_{447} is observed for CT-DNA binding effects only.

The decrease in the absorption of $\text{Ru}(\text{phen})_3^{+2}$ in the presence of CT-DNA indicates that the complex binds to the CT-DNA (figure 5.11). The resulting data (table 5.4) showed that the percent change in A_{447} , in the absence of DNA, between the initial A_{447} and the subsequent A_{447} following the addition of buffer was approximately 7.8%. This corresponds to the change in concentration of the metal complex. The percent change in the A_{447} between the metal complex sample in the absence and the presence of CT-DNA was calculated to be approximately 14.0%. This represents the effect of CT-DNA on the absorption based on binding of the $\text{Ru}(\text{phen})_3^{+2}$ to the DNA. The difference between the pure concentration effects and the CT-DNA plus concentration effects was approximately 6.2%. This represents the effect of CT-DNA only on the absorbance of UV light in a sample of $\text{Ru}(\text{phen})_3^{+2}$. Based on an approximation of absorbances (estimated by following a straight edge from the peak to the y-axis labeled 0.1 and 0.2) in the presence and absence of CT-DNA in the literature (Kelly et al., 1985), the effect of DNA on the absorbance of a sample of $\text{Ru}(\text{phen})_3^{+2}$ under similar conditions was calculated to be approximately 9.1%. Therefore, the results of this experiment confirm that the $\text{Ru}(\text{phen})_3^{+2}$ complex binds to CT-DNA. This method will be useful for application to the analysis of new platinum(IV) tris-substituted complexes to determine potential DNA binding agents.

The absorption spectrum of compound (2) shows λ_{max} to be around 509 nm. A_{509} was less than 0.1 absorbance units. Upon adding CT-DNA in a similar method to that described above, a decrease in A_{509} was suggested. However, these results can not be directly compared to those above because the same amount of DNA was not added (due to a limited supply). According to calculations (Appendix B), 1.8 A_{260} units of CT-DNA is needed for each experiment. This is 11 μL of 23 mM CT-DNA. 33 μL of 10 mM phosphate buffer was added to 5 A_{260} units of CT-DNA in the vial in which it was shipped, but it was difficult to recover all 33 μL from the vial. This experiment should be repeated when more CT-DNA is available.

SECTION 6: FUTURE RESEARCH

Section 6.1: Continued Synthesis

Further research will focus on the synthesis of other Pt(IV) complexes synthesized via scheme 1 using such ligands as listed in figure 1.1. The compounds are to be purified by repeated crystal growth and isolation until only the desired red product remains and the impurities are eliminated. Since the desired red product is more soluble in acetone than the visible impurities, acetone will be used with ether to grow crystals during the purification process. DMSO/ ether will be used to crystallize purified product for X-ray analysis to make the crystals more air stable. However, crystals formed from DMSO are slow growing, if they grow at all, and still are subject to decomposition in air. For this, it is important that the DMSO is saturated with product (only a minute amount of DMSO is needed). Characterization techniques such as IR and NMR analysis, microanalysis, and X-ray crystallography will be applied as complexes are synthesized and purified. While microanalysis data for this type of $M(N-N)_3$ compound may be unreliable in some cases (as was seen for compound (3)), NMR may be employed as an alternate or additional method for compound characterization. A minor hindrance to the synthesis is the small percent yield (which, for future reference, should be calculated for each subsequent synthesis). Practically, several synthesis runs will be necessary for abundant yields^{xxi} to apply these characterization techniques as well as for gel electrophoresis studies.

^{xxi} For example, microanalysis requires several mg of a sample, and while most solutions used for gel electrophoresis are on the order of 1-100 μ M, a significantly greater amount of compound on the order of at least 10 mg is needed for purposes of weighing out the sample to make concentrated stock solutions.

Section 6.2: DNA Binding Studies

Section 6.2A: Gel electrophoresis

To better assess DNA binding, the gel electrophoresis conditions will be meticulously monitored. For example, the running buffer volume will be exactly the same in all apparatus. In addition, the migration of the dye in the loading buffer will be monitored carefully as a check for identical electrophoresis conditions. Since these are preliminary results, more experiments following similar methods are needed to determine reproducibility before generalizations can be solidly supported. Also, the literature should be reviewed for points that may have been overlooked previously.

The topo I assay must be modified so that the enzyme will work and differences can be observed between the relaxed and the supercoiled forms of pBR322. This must be accomplished before any analysis with $M(N-N)_3$ complexes can be continued. The most recent topo I assays conducted during this research project took into consideration longer incubation times and more topo I in the reactions as described by Kellher (1975). The “successful” method will then be applied to the Pt(IV) complexes as they are synthesized to determine the effect of the $M(N-N)_3$ complexes on relaxed and supercoiled DNA.

Section 6.2B: UV-Vis Absorption Spectroscopy

In conjunction with synthesis, characterization, and gel electrophoresis studies, the binding of the new Pt(IV) complexes will be further studied via UV-Vis spectrophotometry and equilibrium dialysis. For UV-Vis studies it is important to determine the absorptivity coefficient (ϵ) at the λ max if the concentration is to be determined. For the preliminary experiment that was run, concentrations were not known exactly.^{xxi} The concentration is needed in order to determine the

^{xxi} The concentrations were known by mass/volume dilutions; however, since the compounds are known to be light sensitive, they may have decomposed over time as they were being exposed to small amounts of light while taking

amount of CT-DNA to add to get a P/D ratio of approximately 40. Therefore ϵ should be determined for compound (2) and other new compounds as they are synthesized and characterized.

Preliminary work with DNA binding studies using UV-Vis spectroscopy has been done with $\text{Pt}(\text{DPK})\text{Cl}_3$ and $\text{Pt}(\text{DPK})(\text{phen})\text{Cl}_2$ by a different method than described here. In these experiments, one major obstacle encountered was the overlapping of the complexes' and DNA's absorbances at their respective λ max (around 260 nm). However, the purified tris-substituted compounds are red/orange, and so have a λ max in the 400 to 550 nm range. Therefore, since the DNA does not have peaks in this range, the synthesized $\text{M}(\text{N-N})_3$ complexes should not overlap with the λ max of DNA.

Equilibrium dialysis is another method of studying the binding of molecules to DNA. In equilibrium dialysis the compound is "equilibrated" with the DNA in semi-permeable tubing. The tubing is permeable to the $\text{M}(\text{N-N})_3$ compounds but not to DNA so the compounds will diffuse through and bind to the DNA until they reach an equilibrium such that in the case of no binding (DNA binding sites are saturated and further binding does not occur) the concentration of the $\text{M}(\text{N-N})_3$ compound inside the tubing is equal to the concentration outside. The solution in which the tubing is immersed is analyzed by UV-Vis spectrophotometry to determine the concentration of the compound remaining. From this, the concentration bound to the DNA can be calculated. In a previous semester, a student conducted preliminary equilibrium dialysis experiments with $\text{Pt}(\text{DPK})\text{Cl}_3$. However, the λ max problems were significant and hindered the collection of meaningful data.

Further studies will also be dedicated to the determination of the mode of DNA interaction. Some methods will be studied by Dr. Jill Granger in the lab of Dr. Jonathan B. Chaires at the University of Mississippi Medical Center during the summer of 1997.

aliquots for experiments. Knowledge of ϵ will allow for determination of the concentration in the cuvette during the experiment.

Section 6.2C: Cell Studies

Because the molecular probes have the potential to alter or stop the processes of transcription and translation, cell studies are in the continuing process of development to determine the probes' effects on cultured normal and tumor cells. These studies are being developed in collaboration with Dr. Robin Davies and Dr. Adele Addington as well as other undergraduate students. One example of further cell-based studies is the Ames test which assesses mutagenicity of compounds. This may aid in determining if these platinum $M(N-N)_3$ complexes are potential chemotherapeutic agents.

Section 6.2D: Compilation of $M(N-N)_3$ characteristics

Once data has been collected concerning the characterization of newly synthesized $Pt(IV)$ complexes, a tabulated summary of characteristics among existing $M(N-N)_3$ analogs will be created to include such characteristics as structural features of the $M(N-N)_3$ compounds (selected bond lengths and angles), mode of DNA interaction, site-specificity of DNA binding, photochemical properties, and potential cytotoxicity of these molecular probes. This summary will allow for better authority when predicting expected interactions of these and related compounds with DNA.

Research will continue on the project in collaboration with Dr. Jill Granger (SBC), Dr. Robert Granger (VMI), Dr. Robin Davies (SBC), Dr. Adele Addington (VMI), Dr. Jonathan B. Chaires (University of Mississippi Medical Center) and by other undergraduate students from Sweet Briar College, Virginia Military Institute, and Randolph Macon Woman's College.

SECTION 7: CONCLUSIONS

Since work began on this project in the spring semester of 1995, $\text{Pt}(\text{DPK})\text{Cl}_3$, $[\text{Pt}(\text{phen})_3](\text{PF}_6)_4$, (**2**) and $[\text{Pt}(\text{DMP})_3]\text{PF}_6$ (**3**) have been synthesized and either fully or partially characterized by IR, microanalysis, and /or X-ray analysis. The $\text{Ru}(\text{phen})_3^{+2}$, $\text{Ru}(\text{dipy})_3^{+2}$ and (**2**) complexes have been used in gel electrophoresis studies to design methods of gel electrophoresis which determine whether the Pt(IV) complex has potential DNA binding activity. Preliminary data suggests the Pt(IV) complexes do bind to DNA, although the complexes have not shown any distinct preference for plasmid DNA or linear DNA (as in λ Hind III). Furthermore, the mode of interaction is uncertain. $\text{Ru}(\text{phen})_3^{+2}$ has been used to confirm UV-Vis spectrophotometric methods result in a decrease in the absorbance at λ max following the method of Kelly et al. (1985). The project is well on its way to the long range goals!

APPENDIX A: Time Line Summary of Research

- Spring 1995: Become familiar with project as a research assistant
- Summer 1995: SBC Honors Fellowship and VMI Summer Undergraduate Chemistry Program
- Research literature
 - Synthesis and characterization trials
 - Synthesize and characterize $\text{Pt}(\text{DPK})\text{Cl}_3$
 - Begin preliminary gel electrophoresis studies
 - Oral presentation for VMI summer program
- Fall 1995: Junior Honors Research
- Gel electrophoresis studies
 - Further characterization of complexes synthesized during the summer
 - Honors Center TIP discussion
- 1996-1997:
- Sept.-Oct: Synthesis and purification of homoleptic $\text{Pt}(\text{IV})$ complex with 4,7- DMP
- November: Send for microanalysis and crystal analysis of above synthesis
- Review summer '96 research and Junior Honors Research to prepare for gel electrophoresis with $\text{Ru}(\text{phen})_3^{+2}$, compound **(2)** and control
- Nov. 15: Thesis proposal due
- December: Begin synthesis & purification of homoleptic $\text{Pt}(\text{IV})$ complex with dipy;
- Redo synthesis with 4,7-DMP
- Dec. 15: Turn in lab notebook and "progress report" to advisor for review
- January: Continue syntheses
- Continue gel studies with $\text{Pt}(\text{IV})$ complexes: topo I studies
- February: Continue J-term objectives
- Begin compiling data: summarize results of gels and characterization of compounds
- March: UV-Vis Absorption Spectroscopy Experiments with $\text{Ru}(\text{phen})_3^{+2}$ and **(2)**
- Wrap up lab research
 - Further compile data and results
- Mar. 20: First draft of thesis due to advisor
- April 5: Presentation at Ewald "Women Succeeding in the Sciences" Conference
- Apr. 9: 2nd draft of thesis due to advisor, second reader
- April 23: Final complete thesis due to advisor, second reader and outside reader
- Apr. 24: Tri-College Consortium Presentation
- Apr. 30: Oral defense of thesis

APPENDIX B: Calculation of pBR322 mM Nucleotides

In performing gel electrophoresis experiments, some methods required that molar concentration of nucleotides (nt) in the pBR322 be calculated to assess the ratio of metal complex to nucleotide DNA since different types of DNA can be used for these studies (i.e., other plasmids). This appendix serves as an example of how to conduct these multi-step calculations.

given: 1000 µg/mL pBR322 stock solution

want: 100 µM nucleotides in 100 µL total volume

? µL stock solution of 1000 µg/mL pBR322 are needed to make a 100 µM nucleotide solution?

$$\begin{aligned} ? \text{ mol pBR322} &= (100 \text{ µM sol'n}) (1 \times 10^{-6} \text{ mol nt/1 µmol nt}) (1 \text{ mol pBR322/ } 8726 \text{ mol nt}) \\ &= 1.146 \times 10^{-8} \text{ mol pBR322} \end{aligned}$$

$$\begin{aligned} ? \text{ µg pBR322} &= (1.146 \times 10^{-8} \text{ mol}) (2.83 \times 10^6 \text{ g/ 1 mol}) (1 \text{ µg/ } 1 \times 10^{-6} \text{ g}) \\ &= 32431.81 \text{ µg pBR322} \end{aligned}$$

$$\begin{aligned} ? \text{ µL pBR322} &= (32431.81 \text{ µg}) (1 \text{ mL/ } 1000 \text{ µg}) (1000 \text{ µL/ } 1 \text{ mL}) = \\ &= 3.243 \times 10^4 \text{ µL pBR322 stock / 1000 mL buffer} \end{aligned}$$

in 100 µL total volume:

$$? \text{ µL pBR322} = 3.243 \text{ µL stock / 100 µL total volume}$$

APPENDIX C: Calculation of P/D

In assessing interaction between DNA and metal complex in the UV-Vis spectroscopy experiments, it is important to determine the appropriate amount of CT-DNA to add to the metal complex solution. This appendix serves as a guide as to how the P/D ratio of molar concentration of phosphates in DNA to dye was calculated.

Given: P/D = 40 = molar concentration phosphates in DNA per molar concentration of dye

$$c = [\text{Ru}(\text{phen})_3^{+2}] = 11.5 \mu\text{M}$$

$$v = 600 \mu\text{L } 10 \text{ mM phosphate buffer in cuvette}$$

$$? \mu\text{mol Ru}(\text{phen})_3^{+2} = (600 \mu\text{L}) (11.5 \mu\text{M}) (1 \text{ L}/10^6 \mu\text{L}) = 0.0069 \mu\text{mol Ru}(\text{phen})_3^{+2}$$

$$? [\text{CT-DNA}] = (0.0069 \mu\text{mol}) (40) = 0.276 \mu\text{mol phosphates}$$

$$? \mu\text{mol CT-DNA} = (0.276 \mu\text{mol phosphates}) (1 \mu\text{mol CT-DNA}/ 26,000 \mu\text{mol phosphates}^*) = 0.0000106 \mu\text{mol CT-DNA}$$

$$? \text{ g CT-DNA} = (0.0000106 \mu\text{mol CT-DNA}) (8.6 \times 10^6 \text{ g DNA}/ \text{mol DNA}) (1 \times 10^{-6} \text{ mol}/ 1 \mu\text{mol}) = 0.000091 \text{ g } (1000 \text{ mg}/1\text{g}) = 0.091 \text{ mg/experiment } (600 \mu\text{L volume})$$

20 units of CT-DNA in 1 mg

$$? \text{ units} = (0.091 \text{ mg}) (20 \text{ units}/ 1 \text{ mg}) = 1.8 \text{ units for each experiment}$$

* There are 2 phosphates for each base pair in DNA.

APPENDIX D: Chemical Characteristics of Platinum and Ruthenium

General

Name	Platinum	Symbol	Pt
atomic number	78	Atomic weight	195.09
Density @ 293 K	21.45 g/cm ³	Atomic volume	9.10 cm ³ /mol
Group	Trans. Met.	discovered	1748

States

state (s, l, g)	s		
melting point	2045.2 K	boiling point	4443 K
Heat of fusion	19.60 kJ/mol	Heat of vaporization	510.0 kJ/mol

Energies

1st ionization energy	870 kJ/mole	electronegativity	2.28
2nd ionization energy	1791 kJ/mole	electron affinity	205.3 kJ/mole
3rd ionization energy	kJ/mole	Specific heat	0.13 J/gK
heat atomization	565 kJ/mole atoms		

Oxidation & Electrons

Shells	2,8,18,32,17,1	electron configuration	[Xe] 4f ¹⁴ 5d ⁹ 6s ¹
minimum oxidation number	0	maximum oxidation number	6
min. common oxidation no.	0	max. common oxidation no.	4

Appearance & Characteristics

structure	fcc: face-centered cubic	color	silvery-white
uses	jewelry, catalysts	toxicity	
hardness	4.3 mohs	characteristics	Inert, ductile

Reactions

reaction with air	none	reaction with 6M HCl	none
reaction with 6M HCl	none	reaction with 15M HNO₃	none
reaction with 6M NaOH	none		

Other Forms

number of isotopes	6	hydride(s)	none
oxide(s)	PtO ₂	chloride(s)	PtCl ₂ PtCl ₄

Radius

ionic radius (2- ion)	pm	ionic radius (1- ion)	pm
atomic radius	139 pm	ionic radius (1+ ion)	pm
ionic radius (2+ ion)	94 pm	ionic radius (3+ ion)	pm

Conductivity

thermal conductivity	71.6 J/m-sec-deg	electrical conductivity	94.34 1/mohm-cm
polarizability	6.5 Å ³		

Abundance

source	nickel ores (sulfides)	rel. abund. solar system	0.127 log
abundance earth's crust	-2.3 log	cost, pure	4700 \$/100g
cost, bulk	1200 \$/100g		

The solar system abundances are relative to silicon. The actual number given is

$\log[(\# \text{ atoms of element} / \# \text{ atoms of silicon}) \times 1E6]$

That is the relative number of atoms of the element in the solar system compared to silicon is scaled by 1E6 and then the log is taken. The relative abundance of silicon is then 6.

In the case of the earth's crust, the number is

$\log(\text{mg element in crust} / \text{kg crustal material})$

That is, the abundances are expressed in parts per million by mass and then put onto a log scale.

General

Name	Ruthenium	Symbol	Ru
atomic number	44	Atomic weight	101.07
Density @ 293 K	12.2 g/cm ³	Atomic volume	8.3 cm ³ /mol
Group	Trans. Met.	discovered	1844

States

state (s, l, g)	s		
melting point	2583.2 K	boiling point	4323 K
Heat of fusion	24.0 kJ/mol	Heat of vaporization	595.0 kJ/mol

Energies

1st ionization energy	711.1 kJ/mole	electronegativity	2.2
2nd ionization energy	1617.1 kJ/mole	electron affinity	101 kJ/mole
3rd ionization energy	2746.9 kJ/mole	Specific heat	0.238 J/gK
heat atomization	643 kJ/mole atoms		

Oxidation & Electrons

Shells	2,8,18,15,1	electron configuration	[Kr] 4d ⁷ 5s ¹
minimum oxidation number	-2	maximum oxidation number	8
min. common oxidation no.	0	max. common oxidation no.	4

Appearance & Characteristics

structure	hcp: hexagonal close pkd	color	silvery-white
uses	catalysts	toxicity	
hardness	6.5 mohs	characteristics	hard

Reactions

reaction with air	none below 800 deg.C	reaction with 6M HCl	none
reaction with 6M HCl	none	reaction with 15M HNO₃	none
reaction with 6M NaOH			

Other Forms

number of isotopes	7	hydride(s)	none
oxide(s)	RuO2 RuO4	chloride(s)	RuCl2 RuCl3

Radius

ionic radius (2- ion)	pm	ionic radius (1- ion)	pm
atomic radius	134 pm	ionic radius (1+ ion)	pm
ionic radius (2+ ion)	pm	ionic radius (3+ ion)	82 pm

Conductivity

thermal conductivity	117 J/m-sec-deg	electrical conductivity	131.579 1/mohm-cm
polarizability	9.6 A^3		

Abundance

source	nickel ores (sulfides)	rel. abund. solar system	0.270 log
abundance earth's crust	-3 log	cost, pure	1400 \$/100g
cost, bulk	\$/100g		

World Wide Web presentation of Chemicool Periodic Table is © Copyright 1996 by David D. Hsu. Some data was provided by and used with the permission of JCE Software and is owned and copyright by the Division of Chemical Education, Inc. Additional data was provided by Perkin-Elmer through Peter Lykos of IIT. The information may not be redistributed without the permission of [David Hsu](#) or [JCE Software](#).

BIBLIOGRAPHY

- (1) Anderson, O.P. "Crystal and Molecular Structure of Tris(1,10-phenanthroline)copper(II) Perchlorate." *J. Chem. Soc., Dalton Trans.* (1973): 1237-1241.
- (2) Atkins, P.W. and Beran, J.A., General Chemistry 2nd ed. W. H. Freeman and Company (1992).
- (3) Ausubel, F.M., Brent, R., Kingston, R.E., Moore, D.D., Seidman, J.G., Smith, J.A., and Struhl, K. (eds.) "Short Protocols in Molecular Biology: A Compendium of Methods from Current Protocols in Molecular Biology." Harvard Medical School. Greene Publishing Associates and Wiley-Interscience.
- (4) Barton, J.K. "Targeting DNA Sites with Chiral Metal Complexes." *Pure and Appl. Chem.* 61 (1989): 563-564.
- (5) Barton, J.K. "Metals and DNA: Molecular Left-Handed Complements." *Science* 233 (1986): 727-734.
- (6) Barton, J.K., Goldberg, J.M., Kumar, C.V., and Turro, N.J. "Binding Modes and Base Specificity of Tris(phenanthroline)ruthenium(II) Enantiomers with Nucleic Acids: Tuning the Stereoselectivity." *J. Am. Chem. Soc.* 108 (1986): 2081-2088.
- (7) Barton, J.K. and Raphael, A.L. "Site-Specific Cleavage of Left-Handed DNA in pBR322 by Λ -tris(diphenylphenanthroline)cobalt(III)." *Proc. Natl. Acad. Sci. USA* 82 (1985): 6460-6464.
- (8) Barton, J.K., Danishefsky, A.T., and Goldberg, J.M. "Tris(phenanthroline)ruthenium (II): Stereoselectivity in Binding to DNA." *J. Am. Chem. Soc.* 106 (1984): 2172-2176.
- (9) Barton, J.K. and Raphael, A.L. "Photoactivated Stereospecific Cleavage of Double-Helical DNA by Cobalt(III) Complexes." *J. Am. Chem. Soc.* 106 (1984): 2466-2468.
- (10) Barton, J.K. "Tris(phenanthroline) Metal Complexes: Probes for DNA Helicity." *J. Biomol. Struct. Dyn.* 1 (1983): 621-632.
- (11) Barton, J.K., Dannenberg, J.J., and Raphael, A.L. "Enantiomeric Selectivity in Binding Tris(phenanthroline)zinc(II) to DNA." *J. Am. Chem. Soc.* 104 (1982): 4967-4969.
- (12) Bonneson, P., Walsh, J.L., Pennington, W.T., Cordes, A.T., and Durham, B. "Six-Coordinate Complexes with 1,10-Phenanthroline Ligands in the Trans Configuration. Preparation of Trans-Bis(1,10-phenanthroline) Ruthenium(II) Complexes and Crystal Structure of Trans-Bis(1,10-phenanthroline) bis(pyridine) Ruthenium(II) Hexafluorophosphate. *Inorg. Chem.* 22 (1983): 1761-1765.

- (13) Bradley, L.J.N., Yarema, K.J., Lippard, S.J., and Essigmann, J.M. "Mutagenicity and Genotoxicity of the Major DNA Adduct of the Anti-tumor Drug *cis*-Diamminedichloroplatinum(II)." *Biochem.* 32 (1992): 982-988.
- (14) Bramwell, V., Crowther, D., O'Malley, S., Swindell, R., Johnson, R., Cooper, E.H., Thatcher, N., and Howell, A. "Activity of JM9 in Advanced Ovarian Cancer: A Phase I-II Trial." *Cancer Treat. Rep.* 69, 4 (1985): 409-416.
- (15) Canty, A.J., Fritsche, S. D., Jin, H., Honeyman, T., Skelton, B. W., and White, A. H. "Oxidation of Organometallic Complexes by Water: Synthesis of Diorgano(hydroxo) platinum(IV) Complexes and the Structure of a Diorgano(aqua) platinum(IV) Complex of Tris(pyridin-2-yl)methanol. $[\text{PtPh}_2\{(\text{py})_3\text{COH-}N,N',N''\}(\text{OH}_2)][\text{NO}_3]_2 \cdot \text{H}_2\text{O}$." *J. Organometallic Chem.* 510 (1996): 281-286.
- (16) Chaires J.B., and Suh, D. "Criteria for the Mode of Binding of DNA Binding Agents." *Bioorg. & Med. Chem.* 3, 6 (1995): 723-728.
- (17) Chaires, J.B. "Inhibition of the Thermally Driven B to Z Transition by Intercalating Drugs." *Biochem.* 25 (1986): 8436-8439.
- (18) Chaney, S.G., Gibbons, G.R., Wyrick, S.D., and Podhasky, P. "An Unexpected Biotransformation Pathway for Tetrachloro-(*d,l-trans*)-1,2-diaminocyclohexane platinum(IV) (Tetraplatin) in the L1210 Cell Line." *Cancer Res.* 51 (1991): 969-973.
- (19) Choi, H., Huang, S., and Bau, R. "Octahedral Complexes of Anti-Cancer Pt(IV)(Cyclohexyldiamine) Agents with 9-Methylguanine." *Biochem. Biophys. Res. Comm.* 156, 3 (1988): 1125-1129.
- (20) Chow, C.S. and Barton, J.K. "Shape-Selective Cleavage of tRNAPhe by Transition Metal Complexes." *J. Am. Chem. Soc.* 112 (1990): 2839-2841.
- (21) Considine, D.M. and Considine, G.D. (eds.) Van Nostrand Reinhold Encyclopedia of Chemistry 4th ed. Van Nostrand Reinhold Company, Inc., (1984): 521.
- (22) Crosby, G. A. "Structure, Bonding, and Excited States of Coordination Complexes." *J. Chem. Ed.* 60 (1983): 791-796.
- (23) a) Del Campo, K., Garcia, S.J., Granger, R.M., and Granger, J.N. "Synthesis and Crystal Structures of $[\text{Pt}(1,10\text{-Phenanthroline})\text{Cl}_4]$ and $[\text{Pt}(\text{Di-2-pyridyl ketal})\text{Cl}_3]$." (Manuscript in Preparation).
 b) Clark, A., Luong, T., Wilson, M., Granger, R.M., Granger, J.N., and Davies R.L. "Synthesis, X-ray studies DNA interactions and cell culture studies of Tris(1,10-Phenanthroline)Pt(IV)." (Manuscript in Preparation).
- (24) Defais, M., Germanier, M., and Johnson, N.P. "Detection of DNA Strand Breaks in *Escherichia coli* Treated with Platinum(IV) Antitumor Compounds." *Chem.-Biol. Interactions* 74 (1990): 343-352.

- (25) Demas, J.N. "Photophysical Pathways in Metal Complexes." *J. Chem. Ed.* 60 (1983): 803-808.
- (26) Eastman, A. "Glutathione-Mediated Activation of Anticancer Platinum(IV) Complexes." *Biochem. Pharmacol.* 36, 23 (1987): 4177-4178.
- (27) Edwards, P.G. "Evidence that Glutathione May Determine the Differential Cell-Cycle Phase Toxicity of a Platinum(IV) Antitumor Agent." *J. Natl. Cancer Institute* 80, 10 (1988): 734-738.
- (28) Elmroth, S.K.C. and Lippard, S.J. "Platinum Binding to d(GpG) Target Sequences and Phosphorothioate Linkages in DNA Occurs More Rapidly with Increasing Oligonucleotide Length." *J. Am. Chem. Soc.* 116 (1994): 3633-3634.
- (29) Fanizzi, F.P., Natile, G., Lanfranchi, M., Tiripicchio, A., Laschi, F., and Zanello, P. "Steric Crowding and Redox Reactivity in Platinum (II) and Platinum (IV) Complexes Containing Substituted 1,10-Phenanthrolines." *Inorg. Chem.* 35 (1996): 3173-3182.
- (30) Fleisher, M.B., Waterman, K.C., Turro, N.J., and Barton, J.K. "Light-Induced Cleavage of DNA by Metal Complexes." *Inorg. Chem.* 25 (1986): 3549-3551.
- (31) Fornefeld, E.J. "Microanalysis and the Organic Chemist: A short practical introduction to microanalysis for organic chemists." Indiana: Midwest Microlab.
- (32) Fornies J., Menjon, B., Sanz-Carrillo, R.M., Tomas, M., Connelly, N.G., Crossley, J.G., and Orpen, A.G. "Synthesis and Structural Characterization of the First Isolated Homoleptic Organoplatinum(IV) Compound: [Pt(C₆Cl₅)₄]." *J. Am. Chem. Soc.* 117 (1995): 4295-4304.
- (33) Friedman, A.E., Kumar, C.V., Turro, N.J., and Barton, J.K. " Luminescence of Ruthenium(II) Polypyridyls: Evidence for Intercalative Binding to Z-DNA." *Nucleic Acids Res.* 19, 10 (1991): 2595-2602.
- (34) Friedman, A.E., Chambron, J.C., Sauvage, J.-P., Turro, N.J., and Barton, J.K. "Molecular "Light Switch" for DNA: Ru(bpy)₂(dppz)⁺²." *J. Am. Chem. Soc.* 112 (1990): 4960-4962.
- (35) Gianini, M., Forster, A., Haag, P., von Zelewsky, A., and Stoeckli-Exans, H. "Square Planar (SP-4) and Octahedral (OC-6) Complexes of Platinum(II) and -(IV) with Predetermined Chirality at the Metal Center." *Inorg. Chem.* 35 (1996): 4889-4895.
- (36) Giedt, D.C. and Nyman, C.J. "62. Tris(ethylenediamine) Platinum(IV) Chloride." *Inorganic Synthesis*; New York: McGraw-Hill, 8 (1966): 239-241.
- (37) Goldstein, B.M., Barton, J.K., and Berman, H.M. "Crystal & Molecular Structure of a Chiral-Specific DNA-Binding Agent: Tris (4,7- diphenyl-1,10 phenanthroline)ruthenium (II)." *Inorg. Chem.* 25 (1986): 842-847.

- (38) Goodisman, J. and Dabrowiak, J.C. "Quantitative Aspects of DNase I Footprinting." *Advances in DNA Sequence Specific Agents*, 1 (1992): 25-49.
- (39) Haq, I., Lincoln, P., Suh, D., Norden, B., Chowdhry, B.Z., and Chaires, J.B. "Interaction of Δ - and Λ -[Ru(phen)₂dppz]²⁺ with DNA: A Calorimetric and Equilibrium Binding Study." *J. Am. Chem. Soc.* 117 (1995): 4788-4796.
- (40) Haworth, I.S., Elcok, A.H., Freeman, J., Rodger, A., and Richards, W.G. "Sequence Selective Binding to the DNA Major Groove: Tris(1,10-phenanthroline) Metal Complexes Binding to Poly(dG-dC) and Poly(dA-dT)." *J. Biomol. Struct. Dyn.* 9,1 (1991): 23-44.
- (41) Hertzbert, R.P. and Dervan, P.B. "Cleavage of Double Helical DNA by (Methidiumpropyl-EDTA)iron(II)." *J. Am. Chem. Soc.* 104 (1982): 313-315.
- (42) Hsu, D. "Chemicoool Periodic Table." JCE Software. Division of Chemical Education, Inc. (1996). netscape address: "<http://the-tech.mit.edu/Chemicoool/elements.html>".
- (43) Kauffman, G.B. and Takahashi, L.T. "59. Resolution of the Tris(1,10-Phenanthroline) Nickel(II) Ion." *Inorganic Syntheses*; New York: McGraw-Hill, 8 (1966):227-232.
- (44) Keck, M. V. and Lippard, S. J. "Unwinding of Supercoiled DNA by Platinum-Ethidium and Related Complexes." *J. Am. Chem. Soc.* 114 (1992): 3386-3390.
- (45) Kellher, W. "Determination of the Number of Superhelical Turns in Simian Virus 40 DNA by Gel Electrophoresis." *Proc. Natl. Acad. Sci. USA* 72, 12 (1975): 4876-4880.
- (46) Kelland, L.R., Murrer, B.A., Abel, G., Giandomenico, C.M., Mistry, P., and Harrap, K.R. "Ammine/ Amine Platinum(IV) Dicarboxylates: A Novel Class of Platinum Complex Exhibiting Selective Cytotoxicity to Intrinsically Cisplatin-resistant Human Ovarian Carcinoma Cell Lines." *Cancer Res.* 52 (1992): 822-828.
- (47) Kelly, J.M. and Murphy, M.J. "A Comparative Study of the Interaction of 5, 10, 15, 20,-Tetrakis (N-Methylpyridinium-4-yl)porphyrin and its Zinc Complex with DNA Using Fluorescence Spectroscopy and Topoisomerisation." *Nucleic Acids Res.* 13, 1 (1985): 167-184.
- (48) Kelly, J.M., Tossi, A.B., McConnell, D.J., and Ohuigin, C. "A Study of the Interactions Some Polypyridylruthenium(II) Complexes with DNA Using Fluorescence Spectroscopy, Topoisomerisation, and Thermal Denaturation." *Nucleic Acids Res.* 13, 17 (1985): 6017-6034.
- (49) Krotz, A.H., Hudson, B.P., and Barton, J.K. "Assembly of DNA Recognition Elements on an Octahedral Rhodium Intercalator: Predictive Recognition of 5'-TGCA-3' by Λ -[Rh(R,R)-Me₂trien)phi]³⁺." *J. Am. Chem. Soc.* 115 (1993): 12577-12578.
- (50) Kumar, C.V., Barton, J.K., and Turro, N.J. "Photophysics of Ruthenium Complexes Bound to Double Helical DNA." *J. Am. Chem. Soc.* 107(1985): 5518-5523.

- (51) Mack, D.P. and Dervan, P.B. "Nickel-Mediated Sequence-Specific Oxidative Cleavage of DNA by a Designed Metallo Protein." *J. Am. Chem. Soc.* 112 (1990): 4604-4606.
- (52) Maniatis, T., Fritsch, E.F., and Sambrook, J. Molecular Cloning: A Laboratory Manual; New York: Cold Harbor Laboratory (1982).
- (53) Mei, H.Y. and Barton, J.K. "Tris(tetramethylphenanthroline)ruthenium(II): A Chiral Probe that Cleaves A-DNA Conformations." *Proc. Natl. Acad. Sci. USA* 85 (1988): 1339-1343.
- (54) Mei, H.Y. and Barton, J.K. "Chiral Probe for A-Form Helices of DNA and RNA: Tris(tetramethylphenanthroline)ruthenium(II)." *J. Am. Chem. Soc.* 108 (1986): 7414-7416.
- (55) Novakova, O., Vrana, O., Kiseleva, V.I., and Brabec, V. "DNA Interactions of Antitumor Platinum(IV) Complexes." *Eur. J. Biochem.* 228 (1995): 616-624.
- (56) Pendyala, L., Cowens, J.W., Cheda, G.B., Dutta, S.P., and Creaven, P.J. "Identification of *cis*-Dichloro-bis-isopropylamine platinum(II) as a Major Metabolite of Iproplatin in Humans." *Cancer Res.* 48 (1988): 3533-3536.
- (57) Pinto, A.L., Naser, L.J., Essigmann, J.M., and Lippard, S.J. "Site-Specifically Platinated DNA, a New Probe of the Biological Activity of Platinum Anticancer Drugs." *J. Am. Chem. Soc.* 108 (1986): 7405-7407.
- (58) Pope, L.E. and Sigman, D.S. "Secondary Structure Specificity of the Nuclease Activity of the 1,10-Phenanthroline-Copper Complex." *Proc. Natl. Acad. Sci. USA* 81 (1984): 3-7.
- (59) Porter, G.B. "Introduction to Inorganic Photochemistry." *J. Chem. Ed.* 60 (1983): 785-791.
- (60) Pyle, A.M., Rehmann, J.P., Meshoyrer, R., Kumar, C.V., Turro, N.J., and Barton, J.K. "Mixed Ligand Complexes of Ruthenium (II): Factors Governing Binding to DNA." *J. Am. Chem. Soc.* 111 (1989): 3051-3058.
- (61) Pyle, A.M., Long, E.C., and Barton, J.K. "Shape-Selective Targeting of DNA by (Phenanthrenequinone diimine)rhodium(III) Photocleaving Agents." *J. Am. Chem. Soc.* 111 (1989): 4520-4522.
- (62) Rahman, A., Roh, J.K., Wolpert-DeFilippes, M.K., Goldin, A., Venditti, J.M., and Wooley, P.V. "Therapeutic and Pharmacological Studies of Tetrachloro(*d,l-trans*) 1,2-diaminocyclohexaneplatinum(IV) (Tetraplatin), A New Platinum Analogue." *Cancer Res.* 48 (1988): 1745-1752.
- (63) Rehmann, J.P. and Barton, J.K. "H NMR Studies of Tris(phenanthroline) Metal Complexes Bound to Oligonucleotides: Characterization of Binding Modes." *Biochem.* 29 (1990): 1701-1709.

- (64) Rendina, L.M., Vittal, J.J., and Puddephatt, R.J. "Stable Organoplatinum (IV) Complexes with Pendant Free Radicals." *Organometallics* 14 (1995): 2188-2193.
- (65) Roat, R.M. and Reedijk, J. "Reaction of *mer*-Trichloro(diethylenetriamine)-platinum (IV) chloride, (*mer*-[Pt(dien)Cl₃]Cl), with Purine Nucleosides and Nucleotides Results in Formation of Platinum(II) as Well as Platinum(IV) Complexes." *J. Inorg.Biochem.* 52 (1993): 263-274.
- (66) Rotondo, E., Fimiani, V., Cavallaro, A., and Ainis, T. "Does the Antitumoral Activity of Platinum(IV) Derivatives Result from Their In Vivo Reduction?" *Tumori.* 69 (1983): 31-36.
- (67) Satyanarayana, S., Dabrowiak, J.C., and Chaires, J. "Tris(phenanthroline)ruthenium(II) Enantiomer Interactions with DNA: Mode and Specificity of Binding." *Biochem.* 32 (1993): 2573-2594.
- (68) Satyanarayana, S., Dabrowiak, J.C., and Chaires, J.B. "Neither Δ- nor Λ-Tris-(phenanthroline)ruthenium(II) Binds to DNA by Classical Intercalation." *Biochem.* 31,39 (1992): 9319-9324.
- (69) Sigman, D. S. "Nuclease Activity of 1,10-phenanthroline-copper ion." *Acc. Chem. Res.* 19 (1986): 180-186.
- (70) Sitlani, A., Dupureur, C.M., and Barton, J.K. "Enantiospecific Palindromic Recognition of 5'-d(CTCTAGAG)-3' by a Novel Rhodium Intercalator: Analogies to a DNA-Binding Proteins." *J. Am. Chem. Soc.* 115 (1993): 12589-12590.
- (71) Tullius, T.D. "I. Metals and Molecular Biology." in Metal-DNA Chemistry; New York: American Chemical Society Symposium Series, 402 (1989): 1-23.
- (72) Tullius T.D. "Chemical 'Snapshots' of DNA: Using the Hydroxyl Radical to Study the Structure of DNA and DNA-Protein Complexes." *TIBS* 12 (1987): 297-300.
- (73) Voet, J. and Voet D. Biochemistry, 2nd ed. John Wiley and Sons, Inc. (1995).
- (74) Vrana, O., Brabec, V., and Kleinwachter, V. "Polarographic Studies on the Conformation of Some Platinum Complexes: Relations to Anti-tumor Activity." *Anti-Cancer Drug Design* 1 (1986): 95-109.
- (75) Wang, J.C. "The Degree of Unwinding of the DNA Helix by Ethidium." *J. Mol. Biol.* 89 (1974): 783-801.
- (76) Waring, M. "Variation of the Supercoils in Closed Circular DNA by Binding of Antibiotics and Drugs: Evidence for Molecular Models Involving Intercalation." *J. Mol. Biol.* 54 (1970): 247-279.
- (77) Yamagishi, A. "Electric Dichroism Evidence for Stereospecific Binding of Optically Active Tris-Chelated Complexes to DNA." *J. Phys. Chem.* 88 (1984): 5709-5713.

- (78) Yarema, K.J., Wilson, J.M., Lippard, S.J., and Essigmann, J.M. "Effects of DNA Adduct Structure and Distribution on the Mutagenicity and Genotoxicity of Two Platinum Anticancer Drugs." *J. Mol. Biol.* 236 (1994): 1034-1048.

VITA

Stephanie J. Garcia of Corpus Christi, TX will graduate from Sweet Briar College, VA in May 1997 receiving her B.S. degree with a Biochemistry/ Molecular Biology major and a Mathematics minor. At Sweet Briar, she was recognized as a Founders' Scholar, the highest scholarship offered at SBC. Honor societies she is a member of include Phi Beta Kappa, Sigma Xi, and Alpha Lambda Delta. Besides working on this project, she has had research experience at the University of Texas Medical Branch in Galveston in Dr. David Gorenstein's lab (1996) and at Armstrong Laboratories, Brooks Air Force Base, San Antonio, TX under the mentorship of Dr. John Taboada (1993) and Dr. Emerson Besch (1992). Stephanie will pursue a Ph.D. from Duke University, NC in the Department of Pharmacology, Integrated Toxicology Program beginning in August 1997.

2482 1174 6

06/13/97

MAB



